

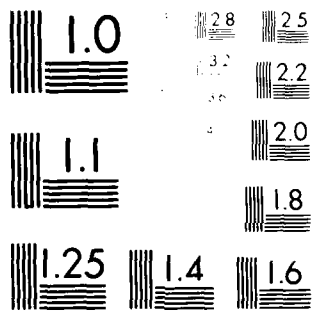
AD-A110 377 NAVAL POSTGRADUATE SCHOOL MONTEREY CA F/6 11/6
THE EFFECTS OF SIMULATED WELDS ON HY-130 CAST AND WROUGHT PLATE--ETC(U)
SEP 81 P E CINCOTTA

UNCLASSIFIED

NL

104
AD-A
110 377

END
DATE
FILMED
02 82
DTIC



MICROCOPY RESOLUTION TEST CHART
NBS 1963-A

②

LEVEL

TH

AD A110377

NAVAL POSTGRADUATE SCHOOL Monterey, California



DTIC
ELECTE
FEB 5 1982
S B

THESIS

THE EFFECTS OF SIMULATED WELDS ON HY-130 CAST AND
WROUGHT PLATE AND WELD METAL MICROSTRUCTURE

by

Paul E. Cincotta

September 1981

Thesis Advisor:

K. D. Challenger

Approved for public release, distribution unlimited.

82 02 04 611

1/10

Unclassified

SECURITY CLASSIFICATION OF THIS PAGE (When Data Entered)

REPORT DOCUMENTATION PAGE		READ INSTRUCTIONS BEFORE COMPLETING FORM
1. REPORT NUMBER	2. GOVT ACCESSION NO. AD-A110377	3. RECIPIENT'S CATALOG NUMBER
4. TITLE (and Subtitle) The Effects of Simulated Welds on HY-130 Cast and Wrought Plate and Weld Metal Microstructure		5. TYPE OF REPORT & PERIOD COVERED Masters Thesis September 1981
		6. PERFORMING ORG. REPORT NUMBER
7. AUTHOR(s) Paul E. Cincotta		8. CONTRACT OR GRANT NUMBER(s)
9. PERFORMING ORGANIZATION NAME AND ADDRESS Naval Postgraduate School Monterey, California 93940		10. PROGRAM ELEMENT, PROJECT, TASK AREA & WORK UNIT NUMBERS
11. CONTROLLING OFFICE NAME AND ADDRESS Naval Postgraduate School Monterey, California 93940		12. REPORT DATE September 1981
		13. NUMBER OF PAGES 61
14. MONITORING AGENCY NAME & ADDRESS (if different from Controlling Office)		15. SECURITY CLASS. (of this report)
		15a. DECLASSIFICATION/DOWNGRADING SCHEDULE
16. DISTRIBUTION STATEMENT (of this Report) Approved for public release, distribution unlimited.		
17. DISTRIBUTION STATEMENT (of the abstract entered in Block 20, if different from Report)		
18. SUPPLEMENTARY NOTES		
19. KEY WORDS (Continue on reverse side if necessary and identify by block number) Simulated Welds, HAZ, HY-130		
20. ABSTRACT (Continue on reverse side if necessary and identify by block number) The microstructure and hardness of simulated welds in HY-130 cast plate, wrought plate and weld filler metal are investigated. The dependence of these quantities on the austenitizing temperature and the tempering provided by subsequent weld passes is also investigated. The use of a tempering parameter, as developed by Hollomon and Jaffe, allows comparison of different tempering times and temperatures. It was found that in the rapid heating cycle of simulated welding that the AC1 and AC3 temperatures are approximately as much as 150 to 170 °F higher than the corresponding temperatures of		

DD FORM 1 JAN 73 1473

EDITION OF 1 NOV 68 IS OBSOLETE
S/N 0102-014-6001

Unclassified

SECURITY CLASSIFICATION OF THIS PAGE (When Data Entered)

← Unclassified

SECURITY CLASSIFICATION OF THIS PAGE (When Data Entered)

the equilibrium phase diagram for this 0.1% C-5.0% Ni steel. Results indicate that cast plate tends to resist tempering more than either the rolled plate or weld metal. Additionally, structures formed at lower austenitizing temperatures temper more readily. Although all three conditions tempered, the cast plate retained a steep hardness and microstructural gradient through the HAZ and consequently is probably more susceptible to a metallurgical notch effect.

Accession For	
DTIC	<input checked="" type="checkbox"/>
NSA	<input type="checkbox"/>
State	<input type="checkbox"/>
Defense	<input type="checkbox"/>
Distribution/	
Availability Codes	
Dist	Special
A	

DTIC
COPY
INSPECTED
2

DD Form 1473
Jan 69
S/N 0102-014-6601

Unclassified
SECURITY CLASSIFICATION OF THIS PAGE (When Data Entered)

Approved for public release, distribution unlimited

The Effects of Simulated Welds on HY-130 Cast
and Wrought Plate and Weld Metal Microstructure

by

Paul E. Cincotta
Lieutenant Commander, United States Navy
B.S., University of California, 1972

Submitted in partial fulfillment of the
requirements for the degree of

MASTER OF SCIENCE IN MECHANICAL ENGINEERING

from the

NAVAL POSTGRADUATE SCHOOL
September 1981

Author:

Paul E. Cincotta

Approved by:

Kenneth D. Chalkey
Thesis Advisor

Larry R. McKelley
Second Reader

J. J. Marto
Chairman, Department of Mechanical Engineering

William M. Jolley
Dean of Science and Engineering

ABSTRACT

The microstructure and hardness of simulated welds in HY-130 cast plate, wrought plate and weld filler metal are investigated. The dependence of these quantities on the austenitizing temperature and the tempering provided by subsequent weld passes is also investigated. The use of a tempering parameter, as developed by Hollomon and Jaffe, allows comparison of different tempering times and temperatures. It was found that in the rapid heating cycle of simulated welding that the AC1 and AC3 temperatures are approximately as much as 150 to 170°F higher than the corresponding temperatures of the equilibrium phase diagram for this 0.1% C-5.0% Ni steel. Results indicate that cast plate tends to resist tempering more than either the rolled plate or weld metal. Additionally, structures formed at lower austenitizing temperatures temper more readily. Although all three conditions tempered, the cast plate retained a steep hardness and microstructural gradient through the HAZ and consequently is probably more susceptible to a metallurgical notch effect.

TABLE OF CONTENTS

ABSTRACT-----	4
LIST OF TABLES-----	6
LIST OF FIGURES-----	7
I. INTRODUCTION-----	9
II. MATERIAL AND PROCEDURE-----	13
III. RESULTS AND DISCUSSION-----	17
IV. CONCLUSIONS-----	23
V. RECOMMENDATIONS-----	24
APPENDIX A: TABLES AND FIGURES-----	25
LIST OF REFERENCES-----	60
INITIAL DISTRIBUTION LIST-----	61

LIST OF TABLES

Table

I.	Material Specifications-----	26
II.	Material Composition-----	27
III.	Experimental Test Matrix-----	29
IV.	Hardness of As-received Material-----	42
V.	Weld Metal Hardness-----	43
VI.	Rolled Plate Hardness-----	44
VII.	Cast Plate Hardness-----	45
VIII.	Effect of Different Tempers-----	57

LIST OF FIGURES

Figure

1. Illustration of Temper Bead and Straight Bead Welding Schemes -----	25
2. Illustration of Weld Metal and Rolled Plate Blank Location -----	28
3. Example of 2000 °F Austenitizing Curve -----	30
4. Example of 1400 °F Austenitizing Curve -----	31
5. Example of 1340 °F Austenitizing Curve -----	32
6. Microstructure at Center of Specimen Austenitized at 1400 °F -----	33
7. Microstructure of As-Received Material -----	34
8. As-quenched Microstructure of Material Austenitized at 1270 °F -----	35
9. As-quenched microstructure of Material Austenitized at 1340 °F -----	36
10. As-quenched Microstructure of Material Austenitized at 1400 °F -----	37
11. As-quenched Microstructure of Material Austenitized at 1500 °F -----	38
12. As-quenched Microstructure of Material Austenitized at 2000 °F -----	39
13. HY-130 Equilibrium Phase Diagram Schematic -----	40
14. HY-130 Rapid Heating Phase Diagram Schematic -----	41
15. Hardness vrs Austenitizing Temperature for Temper Group Q -----	46
16. Hardness vrs Austenitizing Temperature for Temper Group J -----	47
17. Hardness vrs Austenitizing Temperature for Group K -----	48

18.	Hardness vrs Austenitizing Temperature for Temper Group L -----	49
19.	Hardness vrs Austenitizing Temperature for Temper Group M -----	50
20.	Hardness vrs Austenitizing Temperature for Temper Group N -----	51
21.	Hardness vrs Austenitizing Temperature for Temper Group O -----	52
22.	Comparison of Cast Plate Temper Groups K and L -----	53
23.	Comparison of Rolled Plate Temper Groups K and L -----	54
24.	Comparison of Weld Metal Temper Groups K and L -----	55
25.	Rockwell C Indentor -----	56
26.	Comparison of Rolled Plate Temper Groups J and O -----	58
27.	Comparison of Cast Plate Temper Groups J and O -----	59

I. INTRODUCTION

HY-130 is a low carbon, high yield strength (130 ksi) alloy steel with a tempered martensitic structure in the as-delivered condition. It is characterized by its combination of good strength and fracture toughness. The HY-130 steel weldment system evolved from a statistical study conducted by the U.S. Steel Corporation and sponsored by the U.S. Navy. A weldment system is defined as the base metal, weld filler metal, and the weld heat affected zone (HAZ). HY-130 is intended to be a successor to HY-80, the steel presently used by the U.S. Navy for submarine and deep submergence vehicle pressure hulls. The incentive to utilize HY-130 versus HY-80 is the increased strength to weight ratio.

HY-130 is currently available in either cast or wrought product forms. Although suppliers and manufacturing processes for wrought plate have been identified and certified, this is not the case for cast plate. Cast plate has been manufactured by the ESCO Corporation using the argon-oxygen decarburization (AOD) process. Test plates provided to the U.S. Navy have passed mechanical testing, but some have failed the explosion bulge test (EBT). This test is designed to evaluate the toughness of large plates in the as-welded condition. The fracture initiation in these EBT failures has been in the weld HAZ. The effect of welding on the microstructure (and ultimately on the mechanical properties) is extremely complicated in nature, and not thoroughly understood. Each weld pass results in a welding thermal cycle, with the temperature at any given location dependent

upon the distance from the weld bead and the welding parameters. In multi-pass welding, the HAZ may undergo complex heat treatment having experienced repeated thermal cycles. Any pass, however, can "erase" the effects of all previous weld passes if it austenitizes that region. Welding of HY-130 steel, with its high hardenability, tends to produce martensitic structures. Any tempering that occurs due to subsequent passes will reduce the hardness of the as-welded condition, and consequently improve toughness.

Brucker [Ref. 1] reported that the failure of the cast plates in the EBT was not due to an inherent weakness of the plate or manufacturing process, but rather due to the particular welding sequence used. The plates that passed the EBT were welded using a temper bead sequence on both sides. Figure 1 illustrates a temper bead sequence on the top surface, and a straight bead sequence on the bottom. Brucker proposed that a subsequent weld bead tempers previous beads. In both techniques, the last pass is untempered, but in the temper bead sequence it occurs in the weld metal. Since the weld metal generally has lower carbon content than the base plate, an untempered region will not be as hard as the untempered base metal. Thus, in the temper bead sequence the change in hardness in the base metal HAZ is not as steep as in the straight bead sequence. Brucker further hypothesized that a metallurgical notch (a region where a steep strength gradient exists) was created by the straight bead sequence, and that it became the fracture initiation point.

Since the failure of the plate is being ultimately attributed to insufficient tempering, an attempt was made to correlate the amount

of tempering from subsequent weld passes to a tempering parameter, P. Hollomon and Jaffe [Ref. 2] pioneered the work in this area. They developed the following relationship:

$$P = T(c + \log t) \quad \text{eqn I}$$

where P = tempering parameter
T = tempering temperature (absolute)
c = constant dependant upon the steel
t = tempering time

Further work by Grange and Baughman [Ref. 3] found that a value for the constant, c, of 18 (for time in hours) correlated well for a wide range of carbon (.2 to .85%) and alloy (total alloy content less than 5%) steels. Additionally, they reported that the exact value of the constant was not critical as values in the range 16 to 20 served almost equally as well.

Equation I applies to tempering at a constant temperature. Hollomon and Jaffe (Ref. 2), however, also proposed a method for determining the tempering parameter when the temperature during tempering varies, as in welding. This equation follows:

$$P = T \log (\Delta t 10^C + 10^{P_s/T}) \quad \text{eqn II}$$

where Δt = time spent at tempering temperature
 P_s = value of the tempering parameter at
the start of tempering
with other quantities as previously defined

In the case where the initial parameter, P_s , value is zero, it can be seen that equation II approaches equation I, because the second term becomes negligible with respect to the first. By analyzing the work from a weld instrumented with thermocouples which was

performed by Brucker (Ref. 1), Sorek [Ref. 4] reported the tempering parameter for the temper bead sequence. Since the last pass of the straight bead sequence receives no tempering, its tempering parameter value is zero. The purpose of this study, then, is four-fold:

1. To determine the effect of austenitizing temperature during rapid heating on the HAZ microstructure,
2. to determine the effect of tempering on the severity of the metallurgical notch observed by Brucker,
3. to determine the validity of using a tempering parameter in simulating and analyzing an as-welded structure, and,
4. to develop a laboratory procedure to simulate the microstructures present at the various locations in the weld HAZ.

The fourth point is considered important as correlations between properties and microstructures of the HAZ are very difficult to establish due to the steep microstructural gradient that exists in the HAZ. By producing synthetic HAZ structures in bulk specimens, this microstructure/property correlation is made possible.

II. MATERIAL AND PROCEDURE

Table I provides the required chemical composition of the cast and rolled plate and weld metal according to MIL-S-140s. The actual composition of the cast and rolled material used in this work is listed in Table II. No chemical analysis of the as-deposited weld metal was available. However, since it was procured for shipyard work under the specified MIL standard, it is highly probable that the actual composition is extremely close to the specified values. The material used in the experimental work was provided by the Mare Island Naval Shipyard (MINS). The rolled plate (Plate 050310, U.S. Steel Heat 5P4184) and weld metal are the same as that used in Brucker's instrumented weld studies. The cast material is from Plate 6, ESCO Heat No. 36615; this plate passed the EBT.

A test matrix was designed to simulate various locations within a HAZ and various weld bead sequencing techniques. Table III provides the austenitizing temperatures and the experimental tempering temperatures, and times, and their resulting tempering parameter, P. Six groups of seven specimens from each material were heated to six different austenitizing temperatures. The austenitizing temperatures were chosen to span the intercritical temperatures of HY-130. The value of the tempering parameter ranges from zero to a value equal to that for the normal heat treatment cycle for HY-130. The specimens left in the as-quenched condition make up the temper group with a tempering parameter value of zero. Each of the other six groups received the different temper treatments listed in Table III. This

study uses a value of 14.44 (time in seconds) for the constant, c , which is equivalent to the constant used by Grange and Baughman (18 for time in hours), and temperature in degrees Kelvin.

Test specimens were cut from the base plate or weld metal as 1/2-inch by 1/2-inch by 3-inch blanks. Figure 2 provides a schematic showing the location where the weld metal and wrought plate blanks were cut from the welded plate. Blanks from the cast plate were cut with no specified orientation. These blanks then were cut into 1/2-inch cubes. This specimen cross-section was selected as it is large enough to produce mechanical test specimens required by future studies. Every specimen was austenitized individually through the use of a 5 KW induction heater. Various other methods of heating the samples were tried (e.g., salt bath and furnace), but were unacceptable because the peak austenitizing temperature was not obtained quickly enough. In trying to duplicate the thermal cycle of welding, a method of heating that achieved peak temperature in a few seconds was required. This was obtained in all but the highest austenitizing temperature with the induction heater. The peak temperature was obtained in a maximum of about forty seconds in any event. Figures 3, 4, and 5 show typical curves for the 2000, 1400, and 1340 °F austenitizing cycles respectively. The decrease in the heating rate in the 2000 °F cycle is clearly evident. Upon achieving the peak temperature, power to the induction heater was shut off, and the test sample was forced cooled in a jet of air provided by a small blower. Cooling the specimen in the jet of air closely approximated the cooling rate displayed by the instrumented weld. Chromel-alumel thermocouples were welded to the surface of each test cube to monitor the

temperature during the entire process. It is felt that the temperature could be determined within ± 10 °F during the austenitizing process. A chart recorder was used so that a permanent record of the austenitizing process could be maintained.

After all the samples were austenitized, they were separated into groups and tempered according to the schedule presented in Table III. Side-by-side furnaces were used, one set at a much higher temperature than the tempering temperature. The test cubes were placed in the furnace set at the higher temperature. This created a greater temperature differential and allowed the tempering temperature to be reached much more quickly. During this process, the temperature of the specimens was monitored by a digital readout pyrometer. As the tempering temperature was approached, the temper group was moved from the hotter furnace to the tempering furnace and held for the specified time. Tempering was stopped by a water quench.

At the conclusion of the tempering sequence, Rockwell C hardness readings were taken on the face of the cubes where the thermocouple was attached. At least ten hardness readings were taken for each specimen. After throwing out the high and low values, the mean and standard deviation were calculated. If the standard deviation was greater than one point Rockwell C, an additional ten readings were taken, with the same computational technique utilized to obtain a hardness value. Then standard metallographic techniques were employed with a 2% nital etch to prepare the specimens for optical microscopy. All microscopy was performed on central,

external surfaces of the cubes after removing oxidation and decarburization. Additionally, two specimens austenitized to 1400 °F were optically examined in the central region of the cube to determine if a temperature gradient existed during the induction heating.

III. RESULTS AND DISCUSSION

Optical microscopy of the sectioned specimens austenitized at 1400 °F revealed no microstructural gradient. This implies that a nearly uniform temperature existed during the austenitizing process. Figure 6 exhibits the microstructure at the center of the specimen. No microstructural changes through the thickness were observed, and the microstructure is similar to the surface microstructure shown in Figure 10.

Surface optical microscopy performed on the other specimens revealed that they did not austenitize at the equilibrium A1 temperature reported by Zannis [Ref. 5] for HY-130. Examination of Figures 7 through 12 shows this to be the case. Figure 7 is the microstructure of the as-received material. There is no significant change in the microstructure until an austenitizing temperature of 1400 °F is reached, as shown in Figure 10. This analysis is based on the relative amount of the differing types of martensite (i.e., the tempered martensite of the as-received material and the martensite formed upon cooling from the austenitizing temperatures). The newly formed martensite corresponds to the lighter shaded area of the photographs while the tempered martensite of the as-received material appears darker.

The microstructure of the specimens austenitized to the same temperature display similar structures at 1400x, whether from weld, cast, or wrought origin. At lower magnification, however, the structures appear strikingly different. The rolled plate exhibits

banding caused by localized segregation. The weld metal specimens show the HAZ's of different weld beads, and thus different thermal histories are represented in each specimen. In the micrographs for the 1500 °F group (Figure 11), the structure is almost entirely new martensite, and in Figure 12 (austenitizing temperature of 2000 °F), the microstructure is composed entirely of the newly-formed martensite. From this microstructural observation, it appears that the equilibrium phase diagram A1 and A3 temperatures are shifted upward by approximately 150 °F in rapid heating. This effect is shown schematically in Figures 13 and 14. The circles on Figure 13 represent the different austenitizing temperatures of text matrix.

As noted above, a change in the heating rate occurred in specimens austenitized at 2000 °F. The same effect also was noticed in the samples austenitized at 1500 and 1400 °F. This could be caused by either of two reasons: the Curie temperature for HY-130 could have been exceeded with resulting change in magnetic properties causing a decrease in the heating rate; or, alternatively, this could be an indication of reaching the AC1 with the attendant phase change consuming energy previously spent in heating the specimen. This change occurs at approximately 1370 °F. A similar inflection point in the heating curve was noted in attempts to austenitize specimens in a resistance heated furnace. This occurred at approximately 1360 °F. Thus, the inflection in the heating curve probably is caused by the phase change that occurs above the A1 temperature.

Figures 3, 4, and 5 give further proof of the failure of the specimens heated to 1340 °F, or lower, to be austenitized. The change in slope of the 2000 and 1400 °F curves on cooling occurs due to the exothermic transformation to martensite; this happens at approximately 720 °F. This characteristic is not displayed by the 1340 °F curve of Figure 5.

Tables V, VI, and VII present the hardness of the various temper groups, along with their standard deviations. This data also is presented graphically in Figures 15 through 21. One immediate observation is that the cast plate is, in general, harder than the corresponding rolled plate or weld metal. The reason for this is that the cast plate has a slightly higher carbon content (i.e., 0.12% as compared to 0.09% for the rolled plate). Hence, one must take care to ensure that composition variations, as well as processing variations of product forms are considered when ascribing differences in material properties.

It also is interesting to note that the hardness data scatter is much greater for the weld metal than either the cast or wrought plate. This can be explained by the fact that the weld metal used in this study was cut from a multi-pass weld. No attempt was made to limit the 1/2-inch by 1/2-inch by 3-inch blanks to a single bead. Therefore, each weld metal specimen contained zones of different thermal histories. This variation in heat treatment shows up in the generally larger standard deviations for the weld metal hardness readings.

Figures 22, 23, and 24 show a comparison of the two temper groups that have the same tempering parameter value as that of the last four passes of the instrumented weld. Referring to Table III, one can see the difference between the two tempering schemes used to produce

equivalent values of the tempering parameter. The superimposed plots of these two distinct temper groups show good agreement (especially when one considers the scatter bands of the data). The two temper groups that received tempering equivalent to a parameter value of 13,000 did not show as much agreement. It is believed that in the higher temperature group, the time allowed was too short to be sure that this temperature was achieved throughout the specimens.

One further point about the tempering parameter should be discussed. Grange and Haughman [Ref. 3] reported a value for the steel constant valid for a range of steels. HY-130 is slightly outside this range. It is felt, however, that since they also reported that the value of the constant was not too critical, provided it fell within the range of 16 to 20, the use of a constant equivalent to theirs is justified.

All of the curves of hardness versus austenitizing temperature have the same general shape. As is to be expected, the specimens that were austenitized at the highest temperature, implying a complete transformation to the new martensite, were relatively hard. However, the hardness stays fairly constant until the rapid heating AC1 temperature is reached. This can be explained with the help of Figure 25.

This Figure shows the size of the Rockwell C indenter in relation to the microstructure austenitized at 1500 °F. It is clearly evident that the indenter is averaging the hardness of the newly-formed martensite, and the original tempered martensite present in this particular microstructure. According to the lever rule principle, the first austenite to be formed (as the temperature exceeds

the AC1) contains a higher carbon content than the bulk carbon content. Therefore, the resulting martensite should be harder. As the austenitizing temperature increases, the amount of austenite increases; but, as the austenitizing temperature increases, the carbon content of the austenite decreases until the AC3 is reached, and the austenite will contain nominally 0.1% carbon. The hardness of the resulting new martensite should decrease as the austenitizing temperature increases between the AC1 and AC3. Thus, the indenter is, in actuality, measuring an average hardness of the as-received tempered martensite and the newly-formed martensite. Consequently, despite the fact that as the austenitizing temperature increases, the relative amount of new, untempered martensite also increases, the hardness remains constant. At 1200 and 1270 °F, the temperature is not high enough, nor held long enough, to have any significant effect on the hardness of the original tempered martensite. Around 1340 °F, the hardness drops to a minimum due to overtempering of the as-received martensite without the formation of any new martensite.

Table VIII displays the effect of different tempers. The tabulation of the difference in hardness between temper Group J (minimum temper) and Group K (instrumented weld temper) is inconclusive due to the scatter of the data.

For temper Groups J and O (maximum temper), two interesting trends are readily apparent. First it appears that the cast plate resists tempering more than either the rolled plate or weld metal. This is evidenced by the smaller change in hardness between the two temper groups for the cast plate. In other words, for the same tempering

conditions, the rolled plate and weld metal will temper more than the cast plate (as measured by a decrease in the hardness). Second, that the structures formed by intercritical austenitizing (between the AC1 and AC3) temper more easily than those formed by the higher austenitizing temperatures.

Similar results were reported for HY-80 by Kellock, Sollars, and Smith [Ref. 6]. This effect is shown graphically in Figures 26 and 27. The important point to note from these two curves is that although both the cast and rolled plate undergo tempering, the hardness gradient for the cast plate is much steeper than that of the rolled plate after an equal amount of tempering. This implies that even with the temper bead sequence, the cast plate will be more susceptible to the metallurgical notch effect.

Again, it is possible that the differences noted between the cast and rolled plates are due to the composition differences rather than to the difference in processing. Additional testing of more heats of HY-130 is required to separate the effects of processing from composition.

IV. CONCLUSIONS

Based upon the experimental observations and results, the following conclusions are made:

1. The rapid heating phase diagram for HY-130 has A1 and A3 temperatures of approximately 1350 °F and 1550 °F respectively.
2. The cast plate was harder, in general, due to its higher carbon content.
3. The hardness data scatter, as measured by the standard deviation, is much greater for the weld metal than for either the wrought or cast plate. This is due to the inhomogeneity of the as-received material.
4. The use of a tempering parameter is a valid approach to the simulation of weld HAZ's.
5. The cast plate is more resistant to tempering than the rolled plate or weld metal.
6. The martensite formed after heating to the lower austenitizing temperatures tempers more readily than that formed by the higher austenitizing temperatures. This is believed to be due to the higher carbon content of the martensite formed from austenite in the inter-critical temperature range. This is the primary reason for the change in the hardness gradient effected by tempering.
7. Although tempering does occur in the cast plate, its hardness gradient through the HAZ still will be relatively steep in comparison to the rolled plate. Thus, it is more susceptible to the metallurgical notch effect. This may be due to either processing differences or composition differences.

V. RECOMMENDATIONS

The following recommendations are made:

1. Before the HAZ behavior of cast and wrought HY-130 can be compared, more data on the heat-to-heat variations of HAZ properties needs to be developed.
2. Since the carbon content of the martensite formed from inter-critical austenite will be higher than the average carbon content, it is possible that twinned rather than dislocation martensite may form in this region of the HAZ. This deserves further study.
3. The higher carbon content of the intercritical austenite also may result in some retained austenite in these regions of the HAZ. Additional study is needed.
4. The weld simulation treatment process should be used to evaluate the toughness and SCC resistance of these complex micro-structures.
5. Further studies should be conducted to determine a more exact value of the AC1 and AC3 temperatures for HY-130 under rapid heating conditions.

APPENDIX A

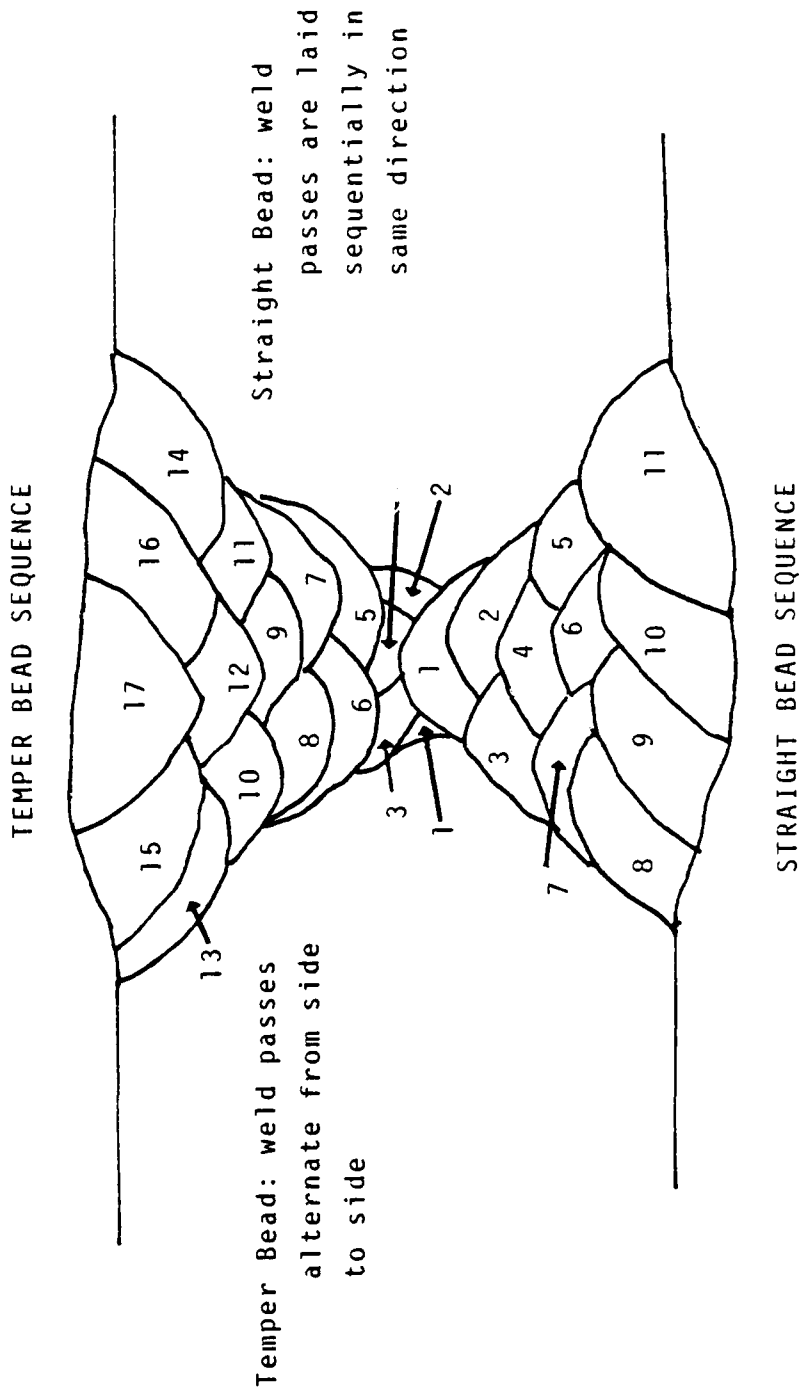


Figure 1. Illustration of temper bead and straight bead welding schemes

TABLE I

MATERIAL SPECIFICATIONS

ELEMENT	WELD METAL *	CAST PLATE	ROLLED PLATE
C	0.09	0.12 MAX	0.12 MAX
NI	2.10	5.25-5.50	4.75-5.25
MN	1.85	0.60-0.90	0.60-0.90
P	0.006	0.01 MAX	0.01 MAX
S	0.007	0.008 MAX	0.01 MAX
SI	0.30	0.20-0.50	0.20-0.50
CR	0.91	0.40-0.70	0.40-0.70
MU	0.54	0.30-0.65	0.30-0.65
TI	0.01	0.02 MAX	0.02 MAX
AL	0.08	0.015-0.035	----
V	----	0.05-0.10	0.05-0.10
CU	----	0.25 MAX	0.25 MAX
U	----	100 PPM	----
H	----	10 PPM	----
N	----	150 PPM	----

* MIL-S-1105

TABLE II

MATERIAL COMPOSITION

ELEMENT	CAST PLATE	ROLLED PLATE
C	0.12	0.90
NI	5.25	4.80
MN	0.77	0.78
P	0.01	0.005
S	0.006	0.007
SI	0.45	0.29
CR	0.55	0.55
MO	0.52	0.54
TI	0.02	0.004
AL	0.034	----
V	0.11	0.06
CU	0.07	0.08
C	43 PPM	----
H	5.5 PPM	----
N	44 PPM	----

CAST PLATE: ROLLED PLATE:
 PLATE 6 PLATE 050310
 ESCG HEAT NC 36612 US STEEL HEAT 5P418

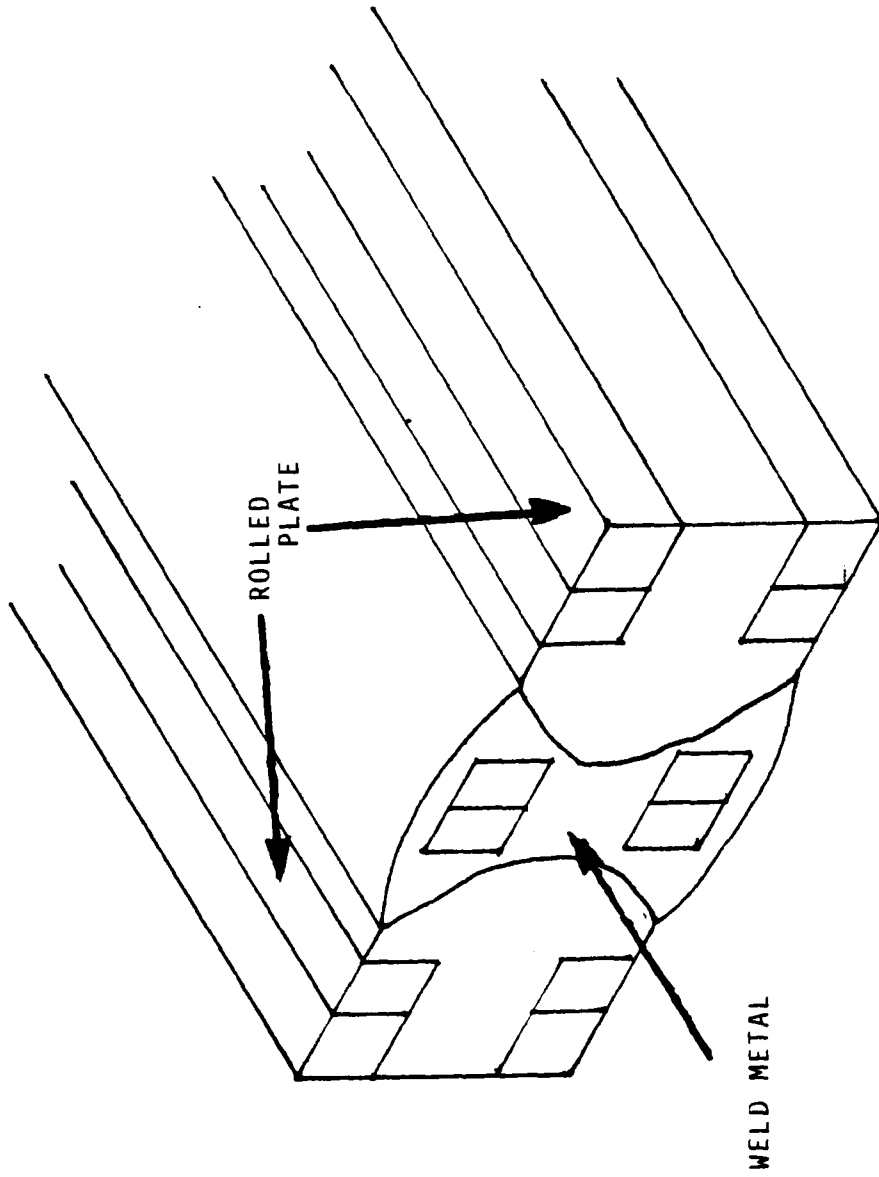


Figure 2. Illustration of weld metal and rolled plate blank location

TABLE III

EXPERIMENTAL TEST MATRIX

AUSTENITIZING TEMPERATURES (F)

1200 1270 1340 1400 1500 2000

TEMPERING HEAT TREATMENT SCHEMES

LETTER DESIGNATION	J	K*	L*	M	N	O	P	Q	R	S	T	U	V	W	X	Y	Z
TEMPERATURE (F)	650	650	800	900	1000	1200											
TIME	41.7 MIN	50.5 MIN	2.4 MIN	45.6 MIN	3 HR	3 HR	3 HR	3 HR	3 HR	3 HR	3 HR	3 HR	3 HR	3 HR	3 HR	3 HR	3 HR

PARAMETER VALUE (P) 11,000 11,013 11,013 13,000 15,000 16,000 16,000 16,000 16,000 16,000 16,000 16,000 16,000 16,000 16,000 16,000 16,000

* TEMPER GROUPS WITH TEMPERIN, PARAMETER EQUAL TO VALUE OF LAST FOUR PASSES OF TEMPER BLEND SEQUENCE IN INSTRUMENTED WELD

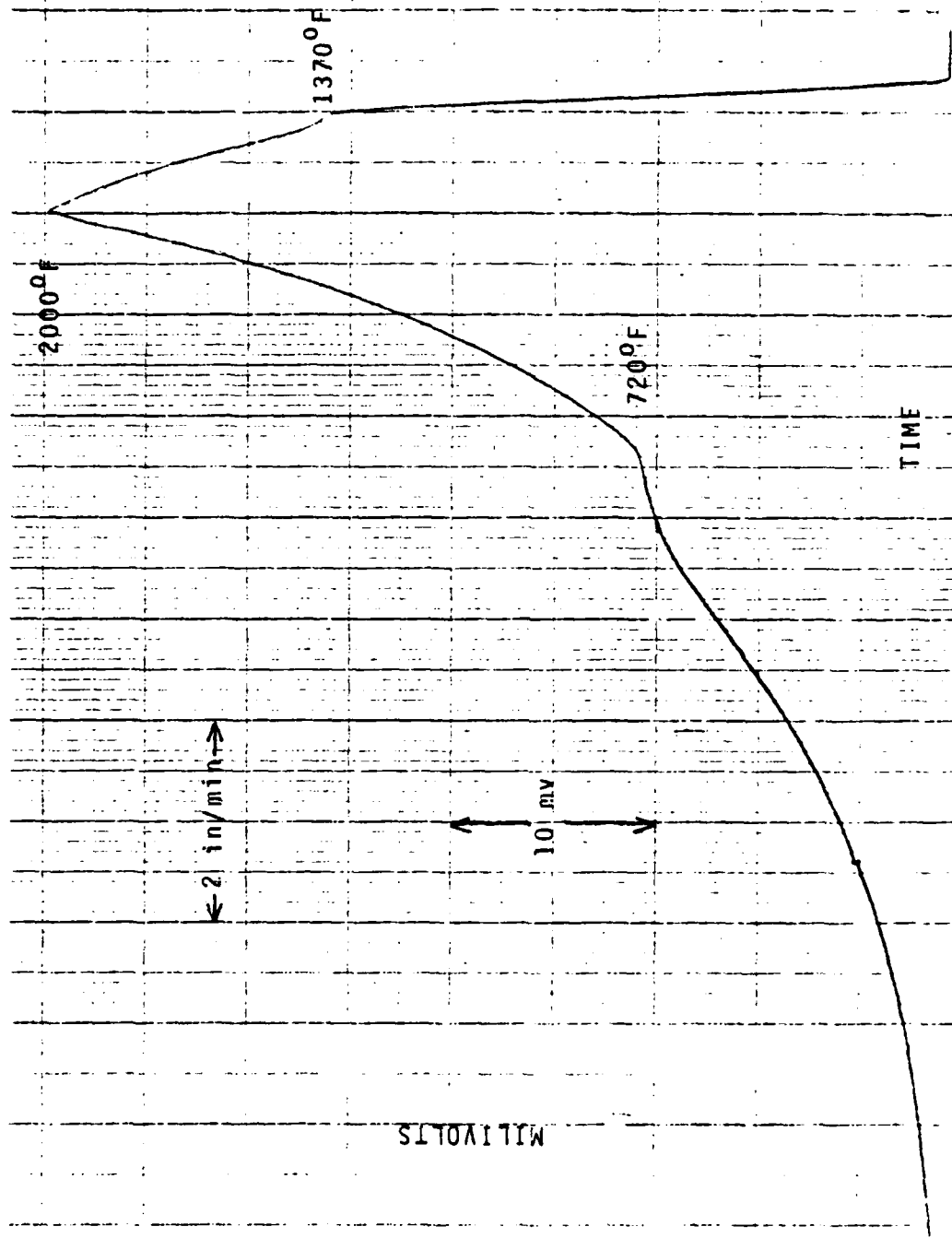


Figure 3. Example of 2000°F austenitizing curve

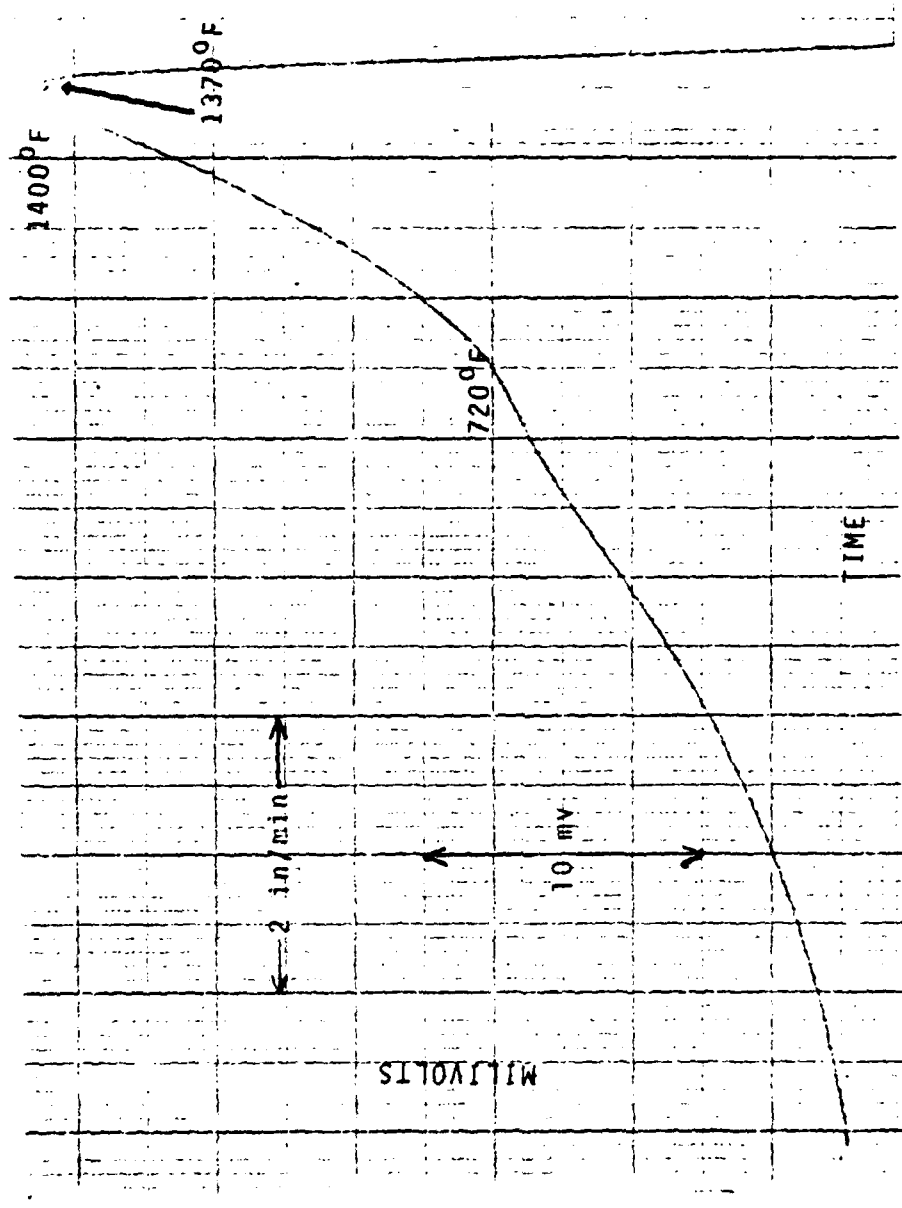


Figure 4. Example of 1400°F austenitizing curve

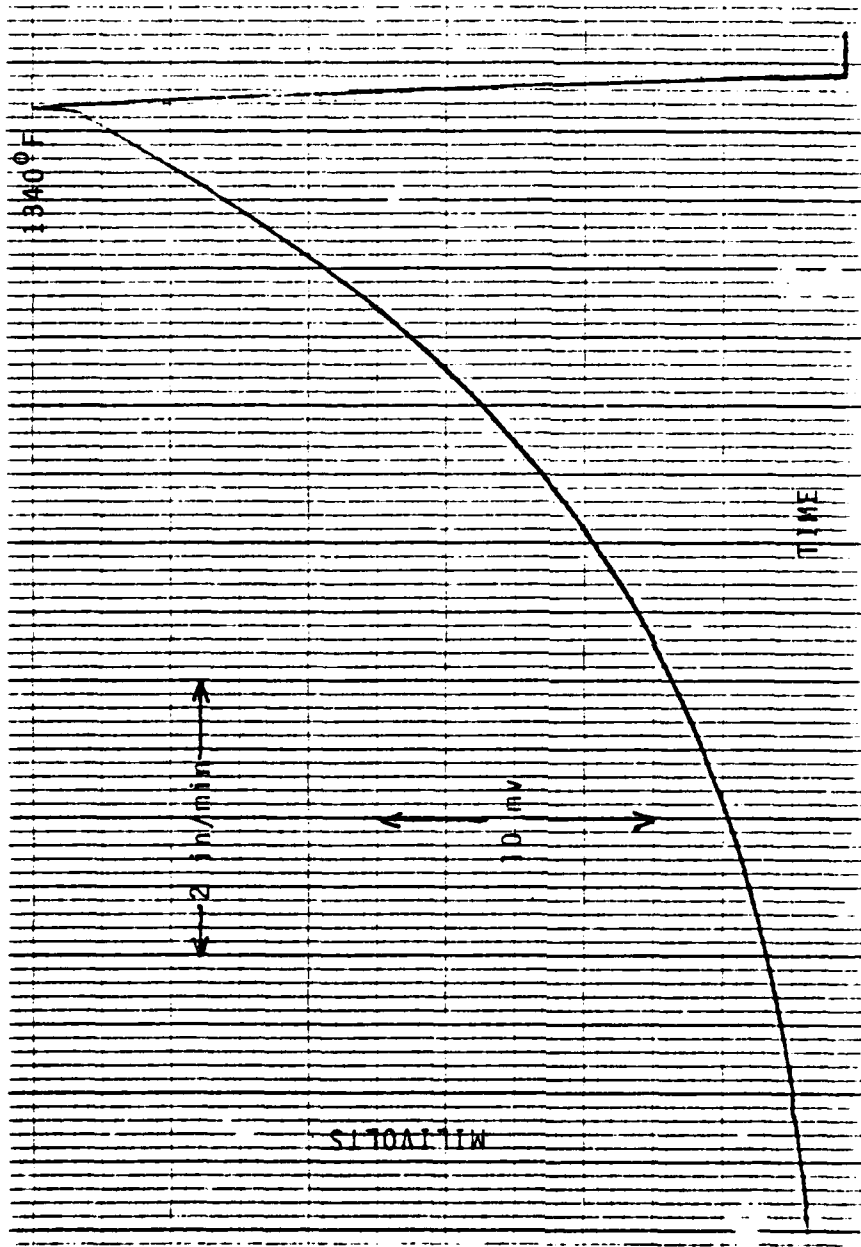
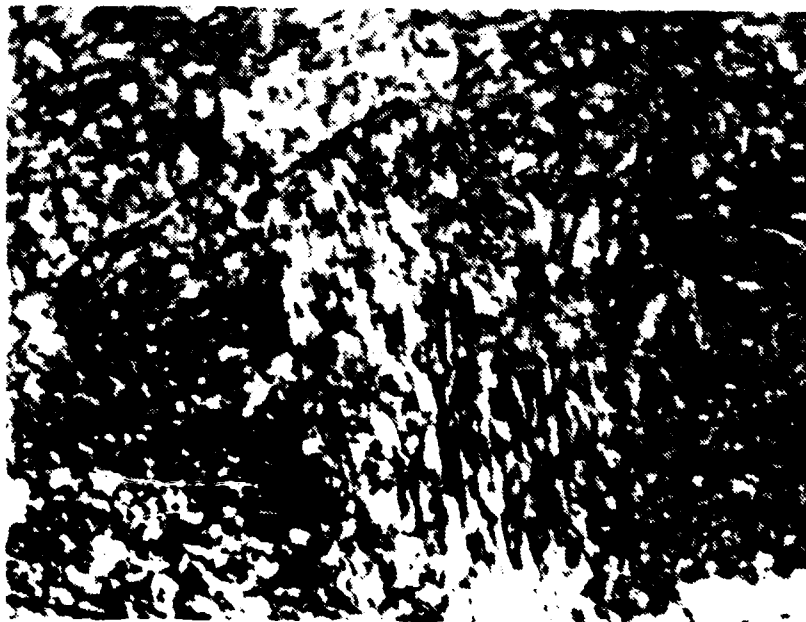


Figure 5. Example of 1340°F austenitizing curve



56x

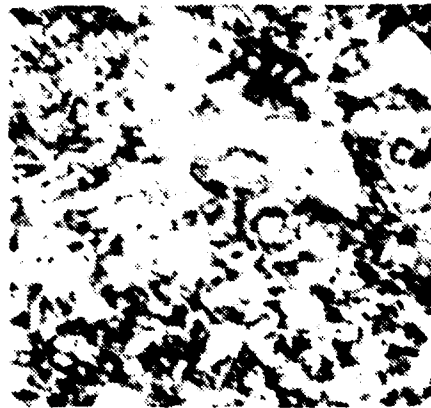


1400x

Figure 6. Microstructure at center of specimen
austenitized at 1400°F

56x

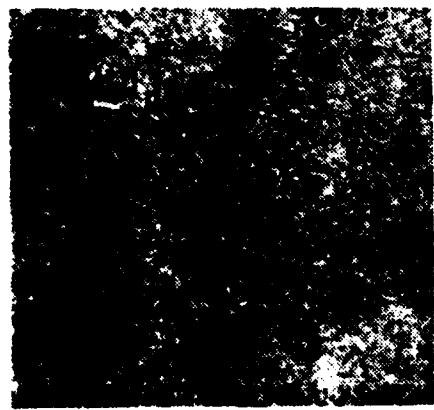
1400x



WELD



ROLLED



CAST

Figure 7. Microstructure of as-received material

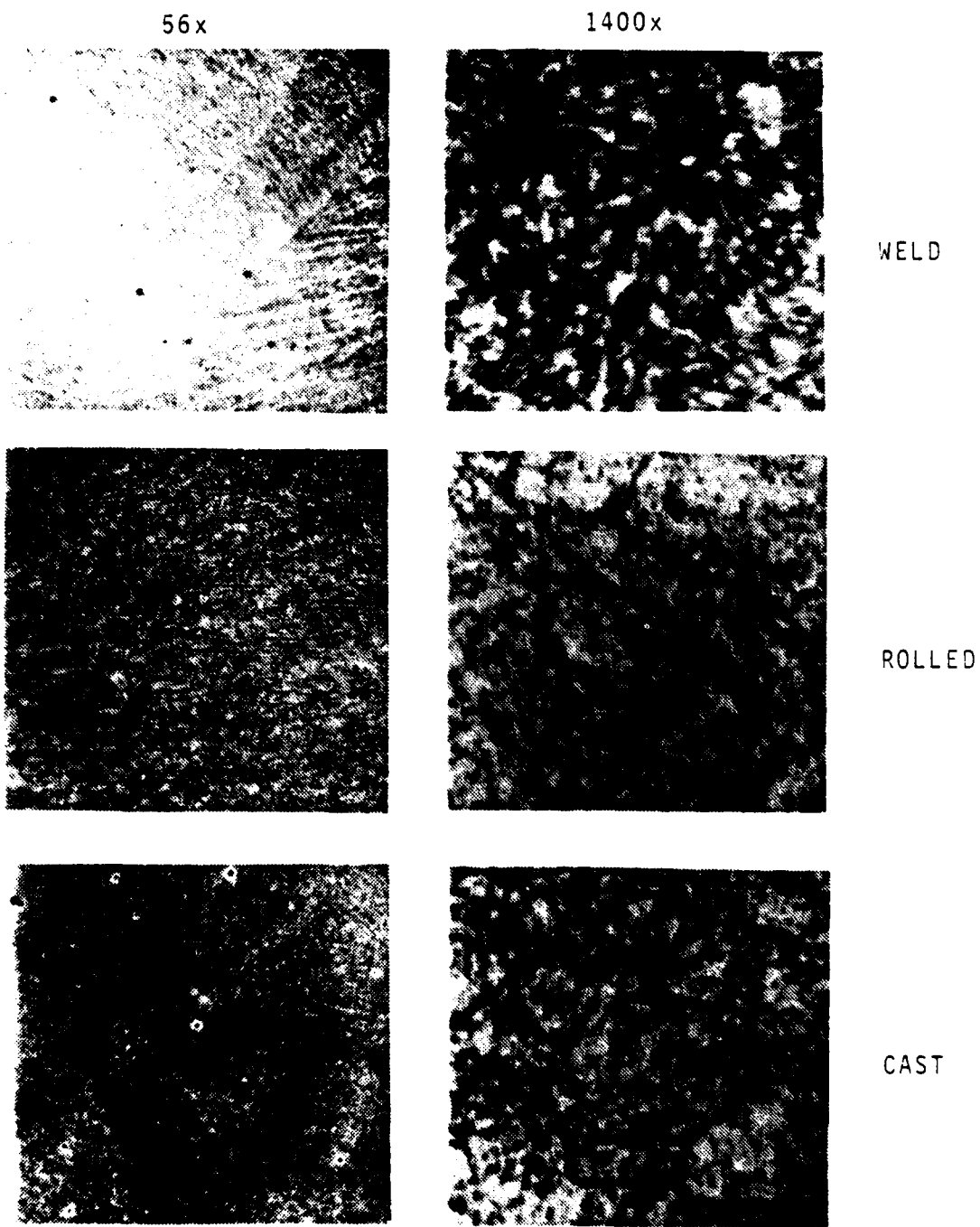
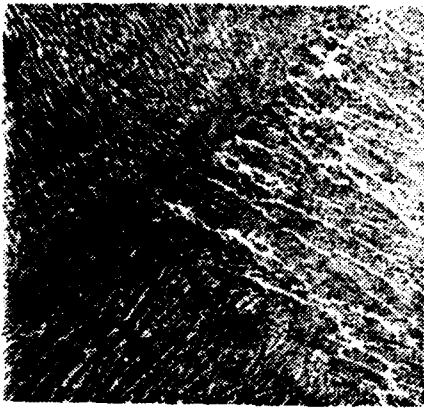


Figure 8. As-quenched microstructure of material
 austenitized at 1270°F

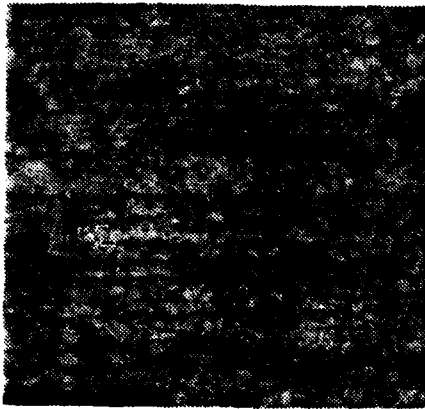
56x



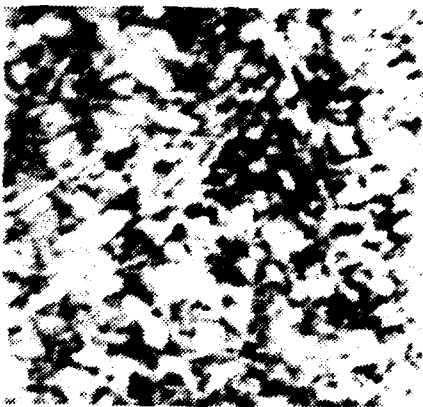
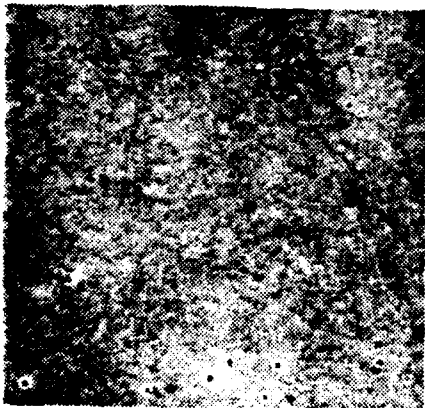
1400x



WELD



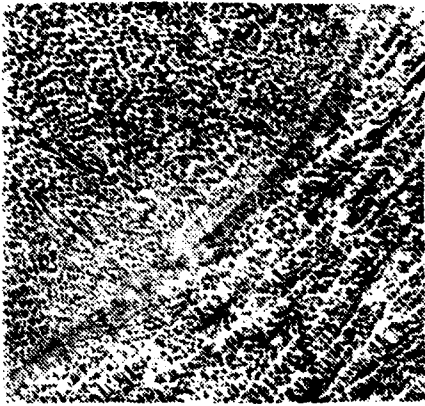
ROLLED



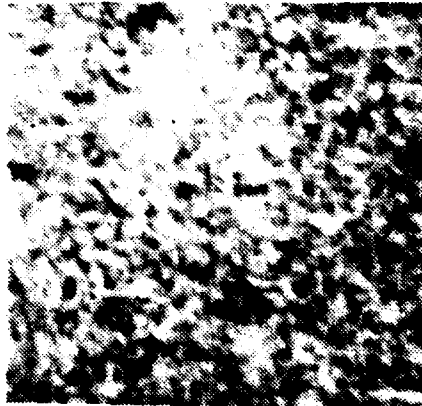
CAST

Figure 9. As-quenched microstructure of material austenitized at 1340°F

56x



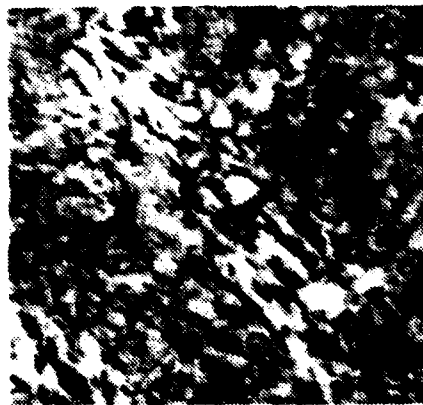
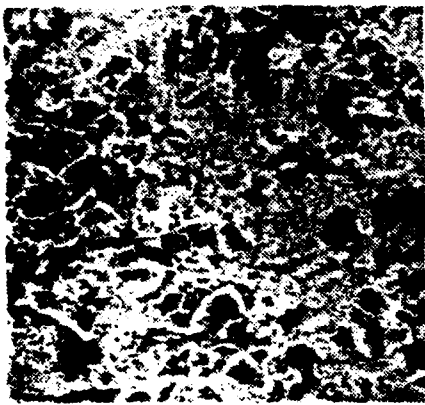
1400x



WELD



ROLLED



CAST

Figure 10. As-quenched microstructure of material
austenitized at 1400°F

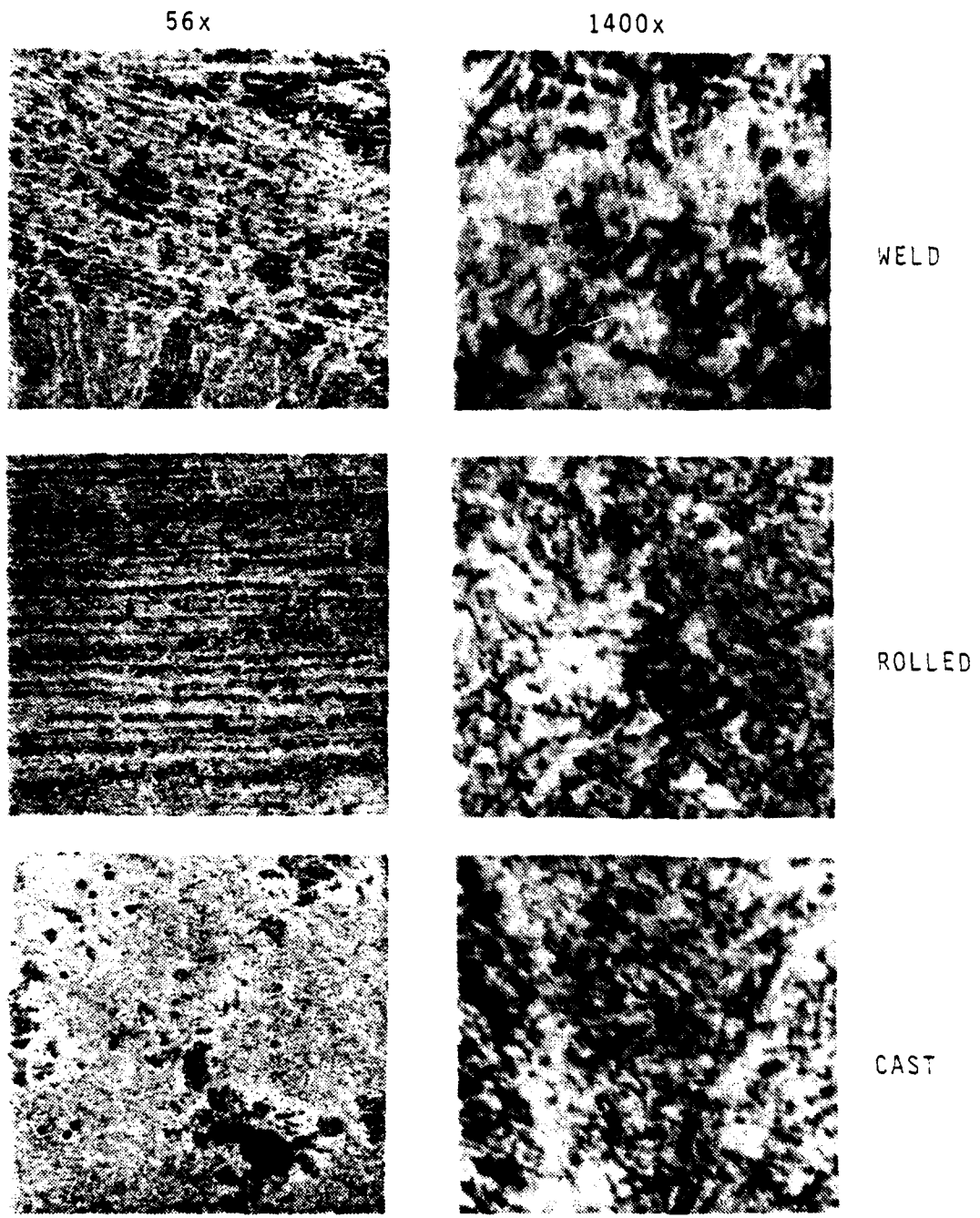
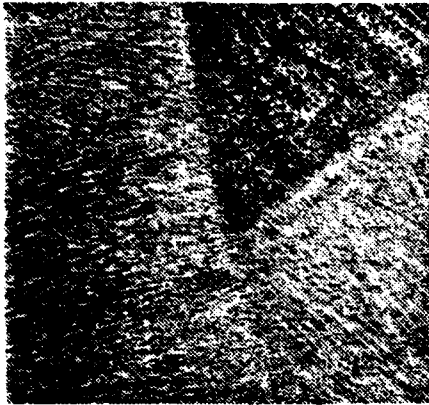
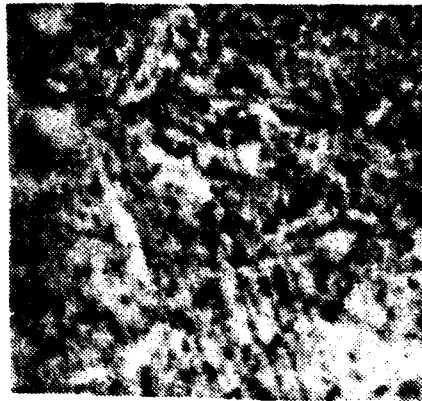


Figure 11. As-quenched microstructure of material austenitized at 1500°F

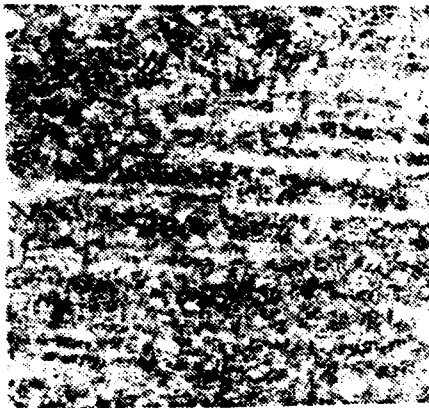
56x



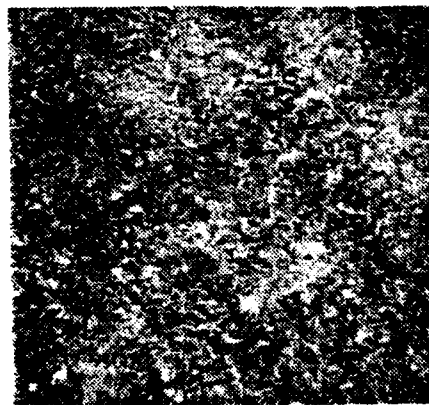
1400x



WELD



ROLLED



CAST

Figure 12. As-quenched microstructure of material
austenitized at 2000°F

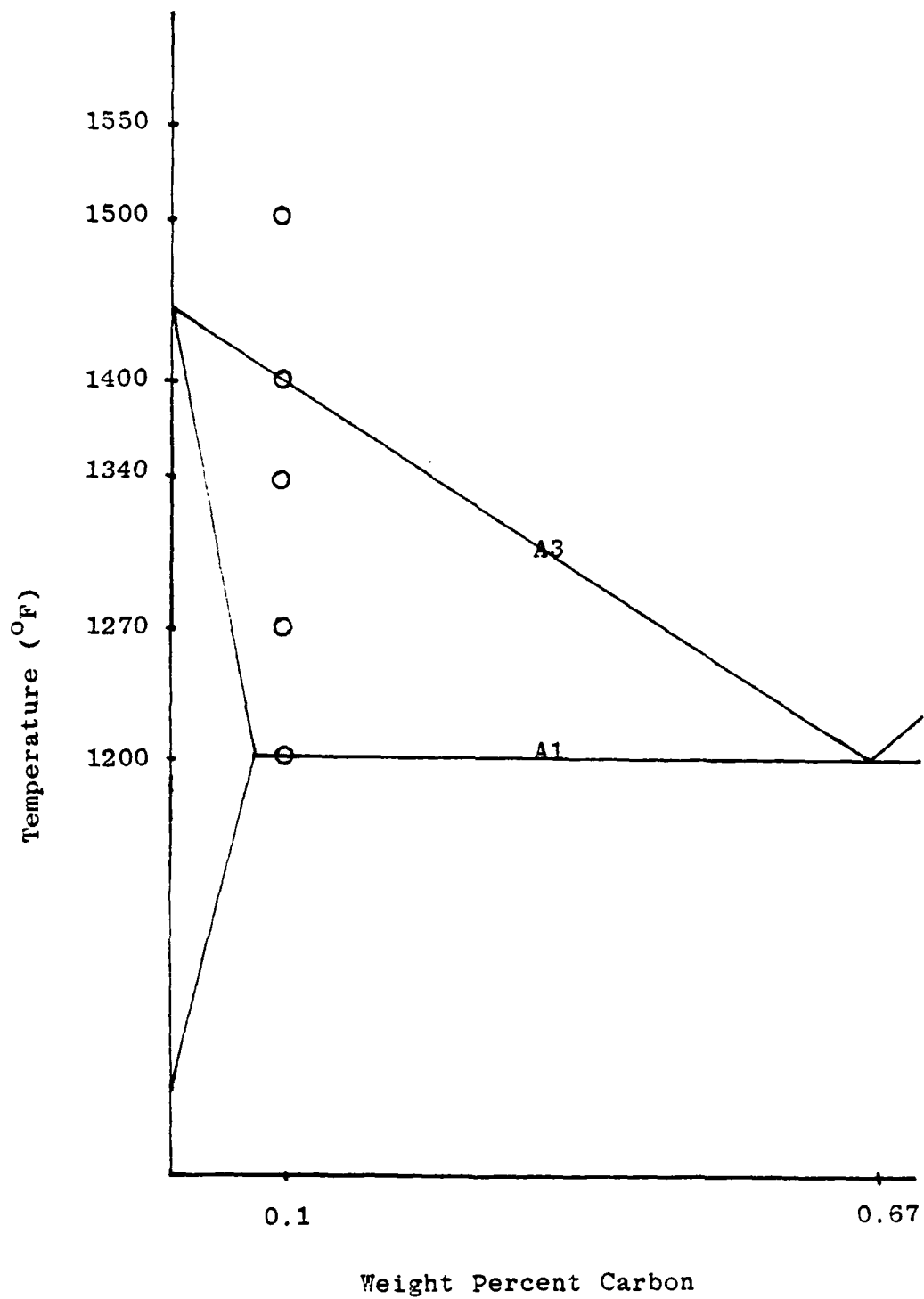


Figure 13. HY-130 equilibrium phase diagram schematic

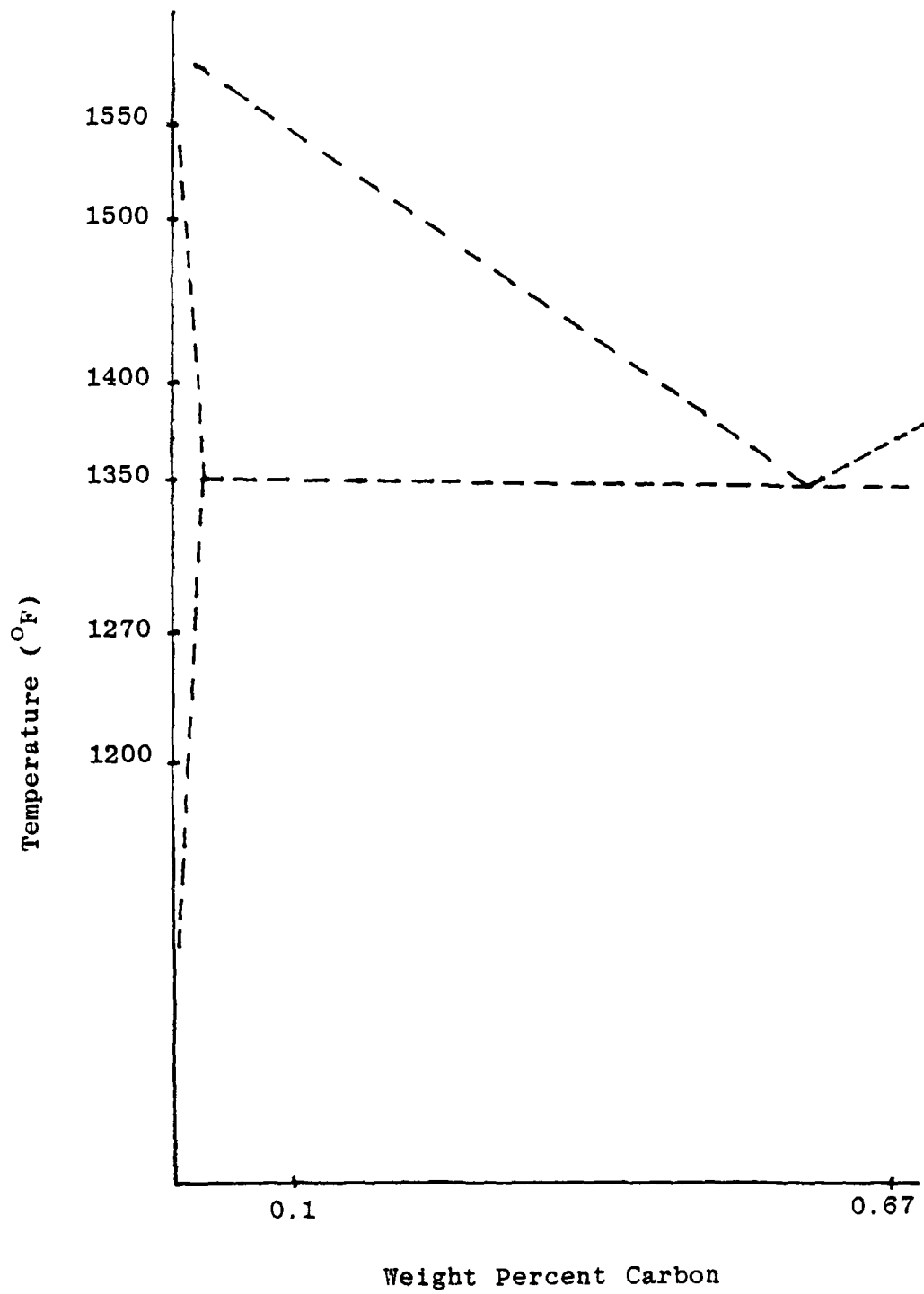


Figure 14. HY-130 rapid heating phase diagram schematic

TABLE IV

HARDNESS IN AS-FECLIVED MATERIAL
(ROCKWELL C)

ROLL METAL	ROLLED PLATE	CAST PLATE
30.5 (1.8)	33.1 (0.3)	32.7 (0.2)

NOTE: NUMBERS IN PARENTHESES ARE
STANDARD DEVIATIONS

TABLE V

WELD METAL HARDNESS
(ROCKWELL C)

TEMPERING GROUP	AUSITIZING TEMPERATURE (F)				
	1200	1270	1340	1400	1500
Q	32.6 (1.7)	31.9 (1.1)	27.1 (0.8)	32.7 (0.8)	33.5 (1.3)
	25.7 (1.7)	22.7 (0.3)	23.2 (0.3)	31.1 (2.0)	30.0 (3.0)
K	31.1 (1.5)	31.7 (1.1)	31.5 (1.1)	35.7 (0.7)	38.3 (0.7)
	27.8 (2.8)	30.7 (1.3)	32.7 (1.3)	32.0 (0.6)	32.2 (1.2)
M	31.4 (1.4)	32.5 (1.1)	30.1 (1.9)	35.9 (1.6)	37.1 (1.1)
	32.5 (0.4)	32.2 (1.1)	29.8 (1.4)	32.2 (0.3)	33.3 (0.7)
P	28.7 (0.8)	27.3 (1.1)	27.3 (0.3)	27.2 (1.2)	31.0 (0.3)
					35.9 (0.7)

NOTE: HARDNESS TO PARTICLES ARE STANDARD DEVIATIONS

TEMPER GROUP LETTER CODES AS SPECIFIED IN TABLE III

TABLE VI

TEMPERATURE GROUP	ROLLED PLATE HARDNESS (ROCKWELL C)				
	AUSPHERITIZING TEMPERATURE (F)				
	1200	1270	1300	1400	1500
Q	30.0 (0.9)	29.8 (0.6)	29.7 (0.6)	30.2 (0.8)	30.7 (0.9)
J	30.5 (1.0)	30.0 (0.6)	29.9 (0.5)	30.2 (1.4)	30.5 (0.5)
K	30.7 (0.7)	29.5 (0.7)	29.3 (0.7)	30.7 (0.7)	31.1 (0.3)
L	30.2 (1.0)	29.9 (1.2)	29.1 (0.5)	30.9 (1.7)	31.2 (1.0)
M	30.2 (0.6)	29.3 (1.0)	29.7 (0.3)	30.5 (0.6)	30.1 (0.8)
N	29.6 (0.8)	29.5 (0.5)	30.3 (0.5)	30.6 (1.0)	30.2 (0.3)
O	29.9 (1.1)	29.6 (0.6)	29.7 (0.6)	30.4 (2.1)	30.9 (0.4)

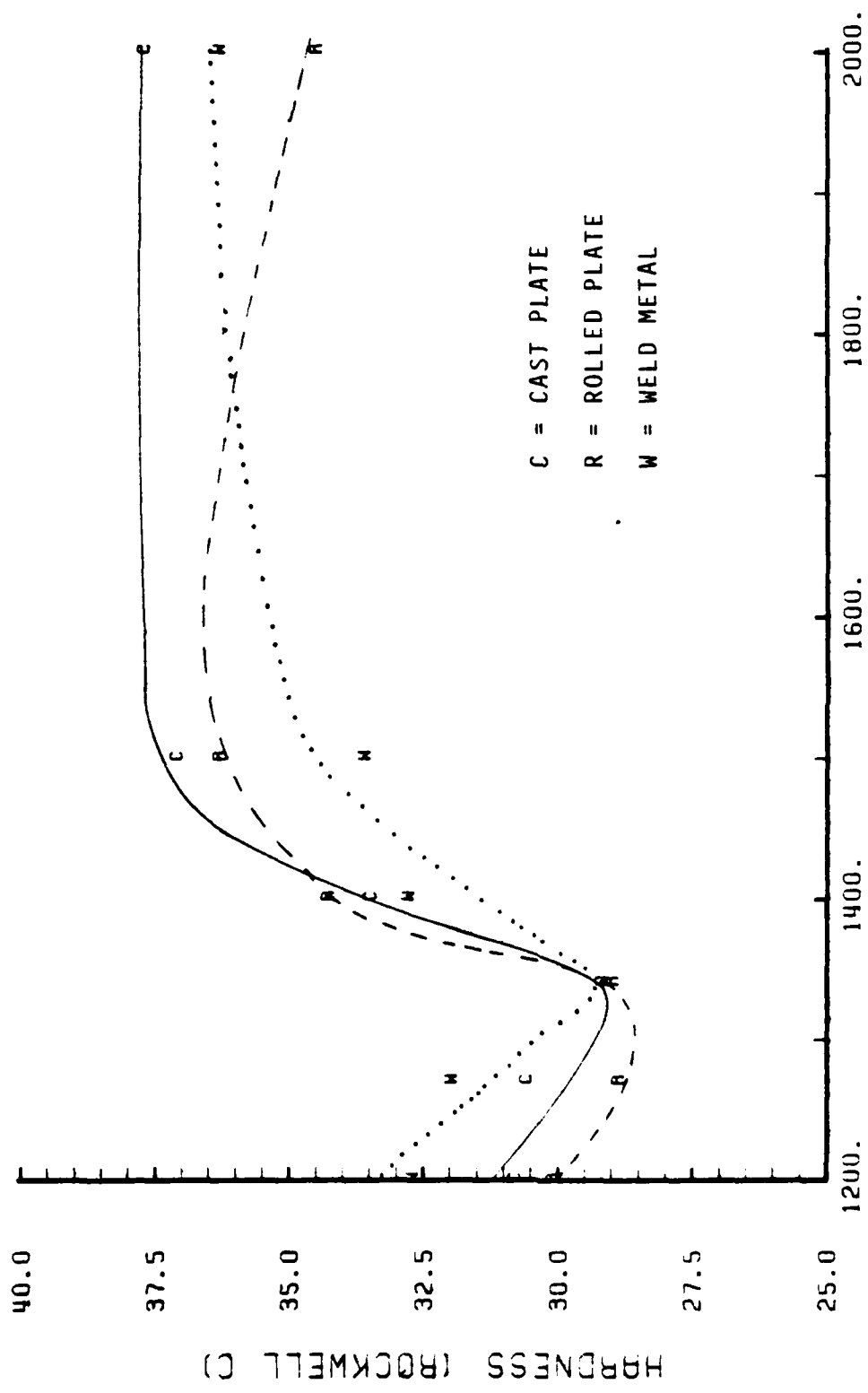
NOTE: NUMBERS IN PARENTHESES ARE STANDARD DEVIATIONS.
TEMPERATURE LETTER CODES AS SPECIFIED IN TABLE III

TABLE VII

CAST PLATE HARDNESS
(ROCKWELL C)

TEMPERING SETUP	AGEING TEMPERATURE (1)					
	1200	1270	1340	1400	1500	2000
G	30.7 (0.6)	30.5 (1.0)	29.1 (2.1)	33.4 (2.6)	37.0 (1.6)	37.5 (0.5)
J	30.7 (1.0)	31.5 (0.9)	31.2 (0.9)	37.0 (1.6)	37.0 (1.5)	37.5 (1.5)
K	30.2 (0.4)	30.6 (0.8)	30.1 (0.6)	36.5 (0.6)	36.4 (0.5)	36.7 (0.5)
L	31.5 (0.6)	29.2 (0.6)	31.6 (0.4)	35.5 (0.9)	38.9 (0.5)	38.5 (0.5)
M	31.6 (0.4)	29.1 (2.2)	30.8 (0.7)	35.7 (0.4)	35.7 (1.0)	35.1 (0.5)
N	30.7 (0.6)	29.0 (1.4)	28.7 (0.5)	37.7 (0.7)	37.7 (0.5)	38.0 (0.7)
O	29.0 (0.7)	27.6 (1.0)	30.1 (0.6)	34.6 (0.4)	38.1 (0.5)	38.7 (1.5)

TABLE: NUMBERS IN PARENTHESES ARE STANDARD DEVIATIONS
TEMPERATURE LETTERS ARE AS SPECIFIED IN TABLE III



AUSTENITIZING TEMP (F) P = ZERO (Q)
 Figure 15. Hardness vs austenitizing temperature for temper group Q

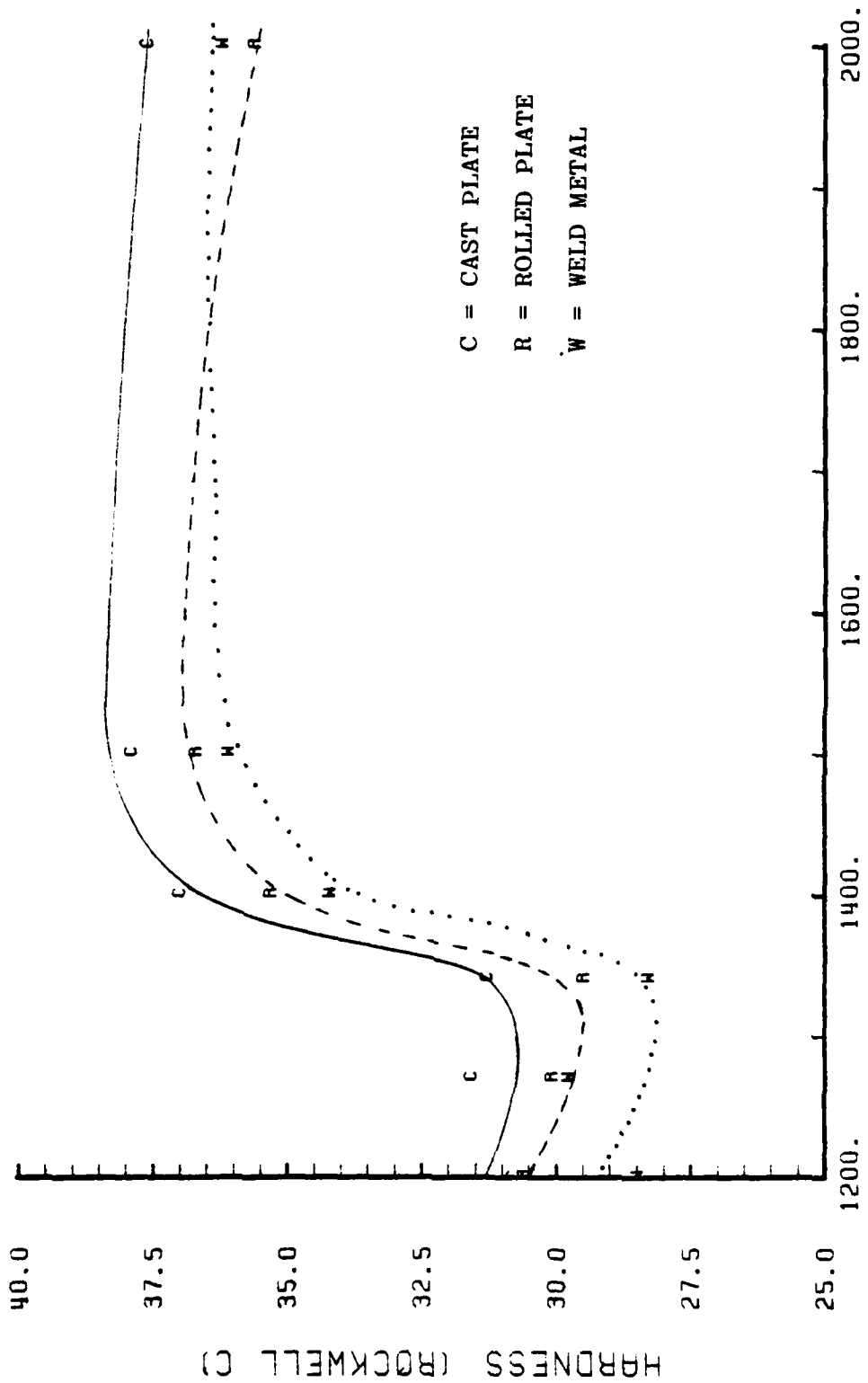
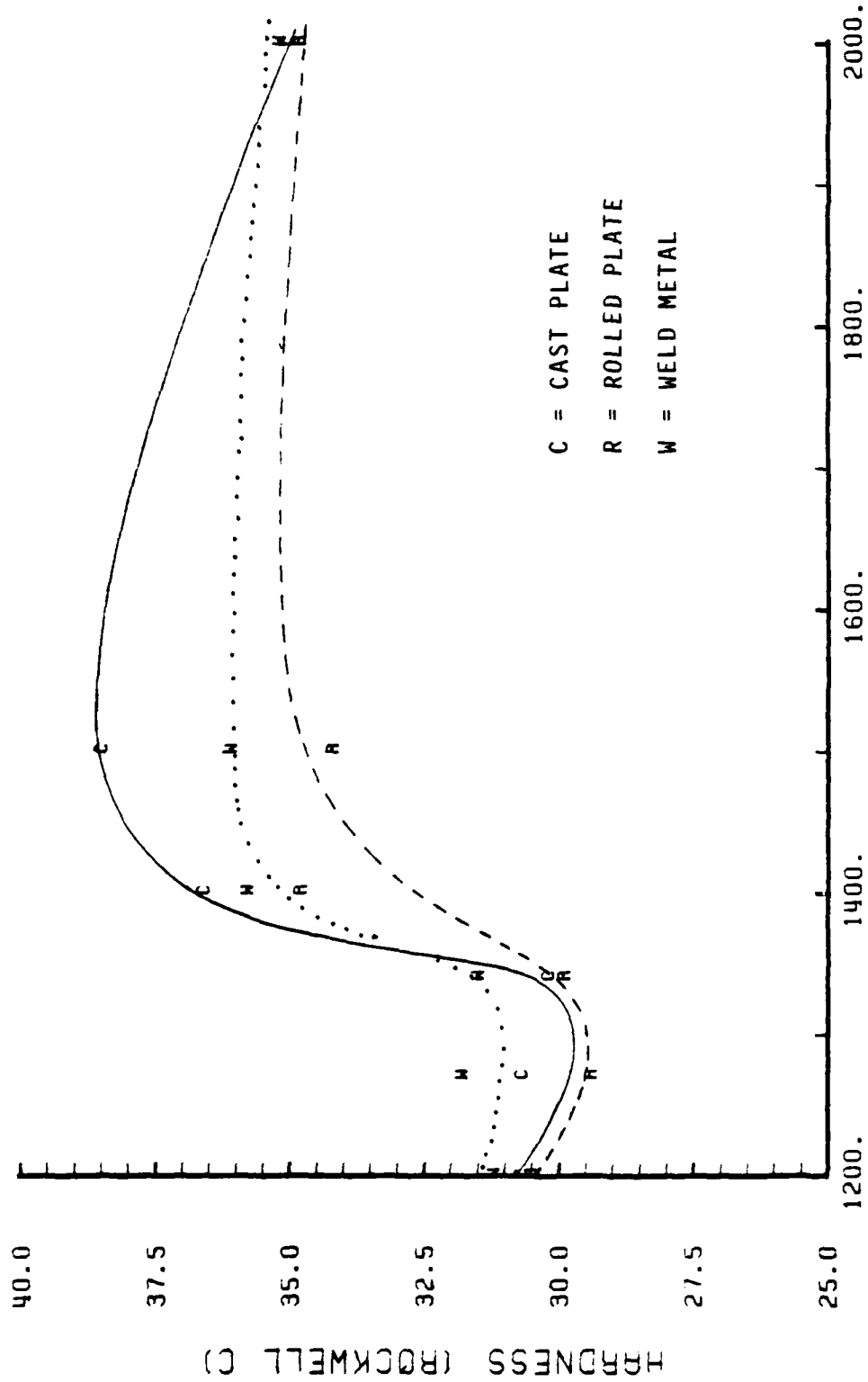


Figure 16. Hardness vs austenitizing temperature for temper group J



AUSTENITIZING TEMP (F) P = 11,613 (K)

Figure 17. Hardness vrs austenitizing temperature for temper group K

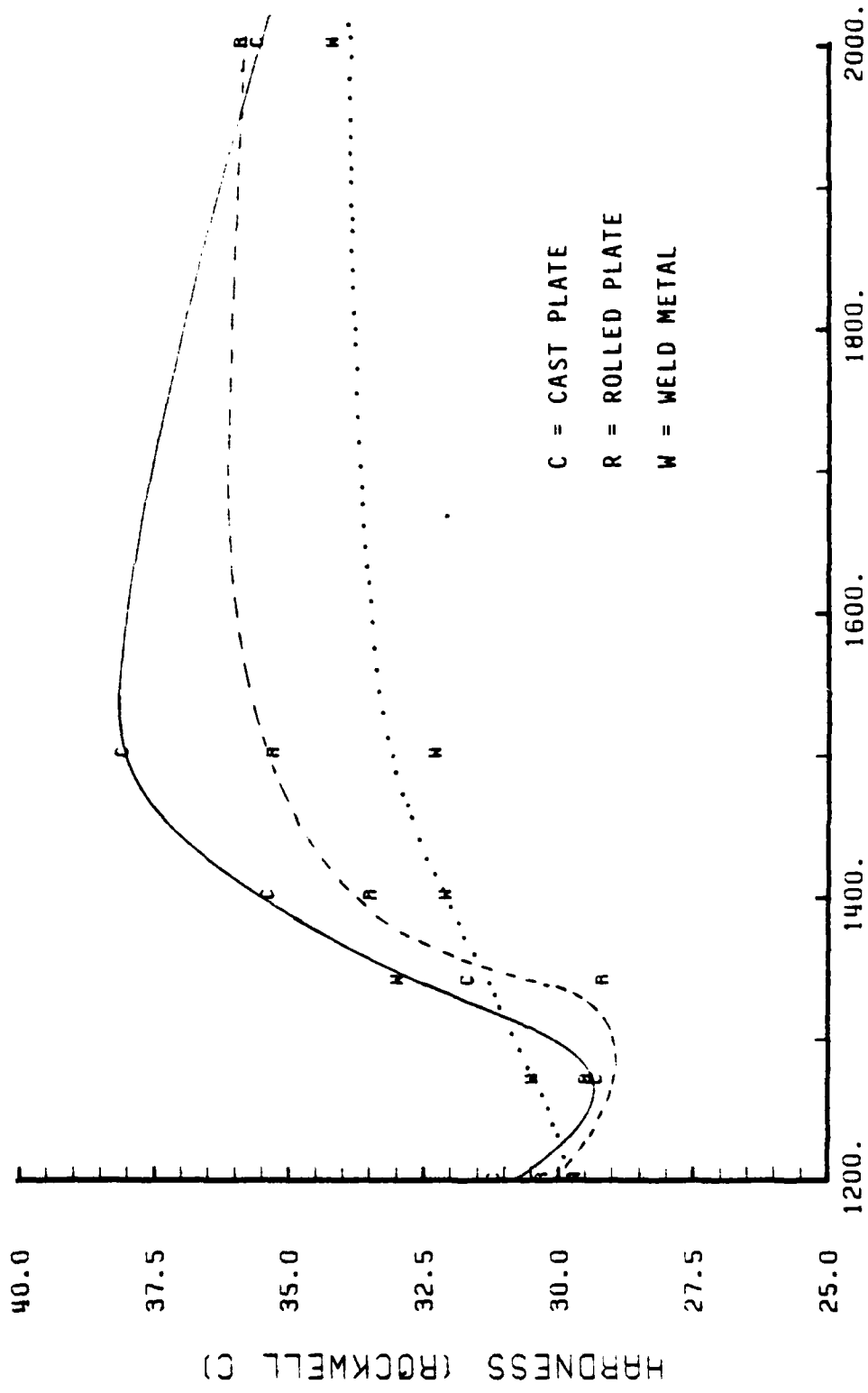
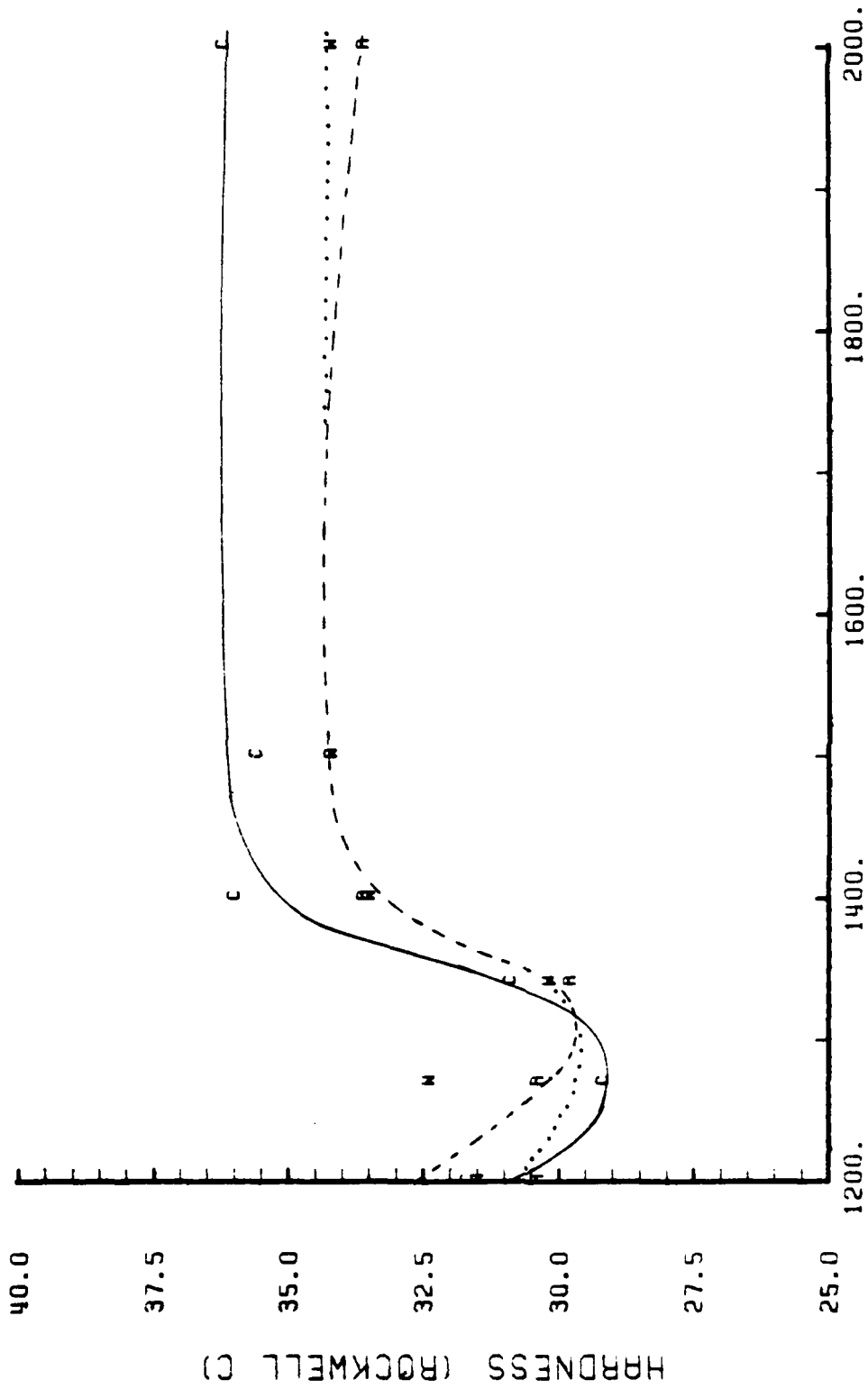
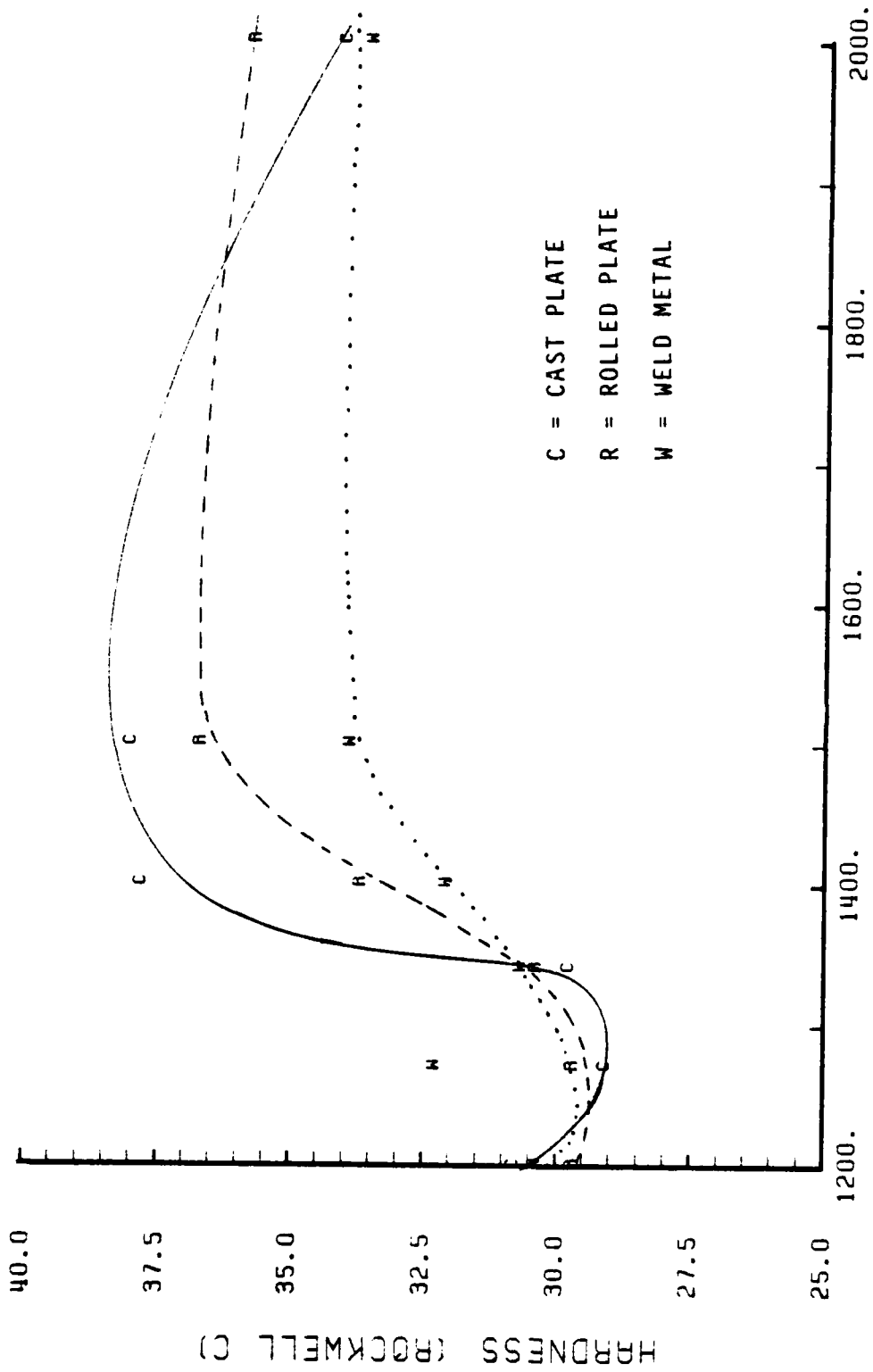


Figure 18. Hardness vrs austenitizing temperature for temper group L



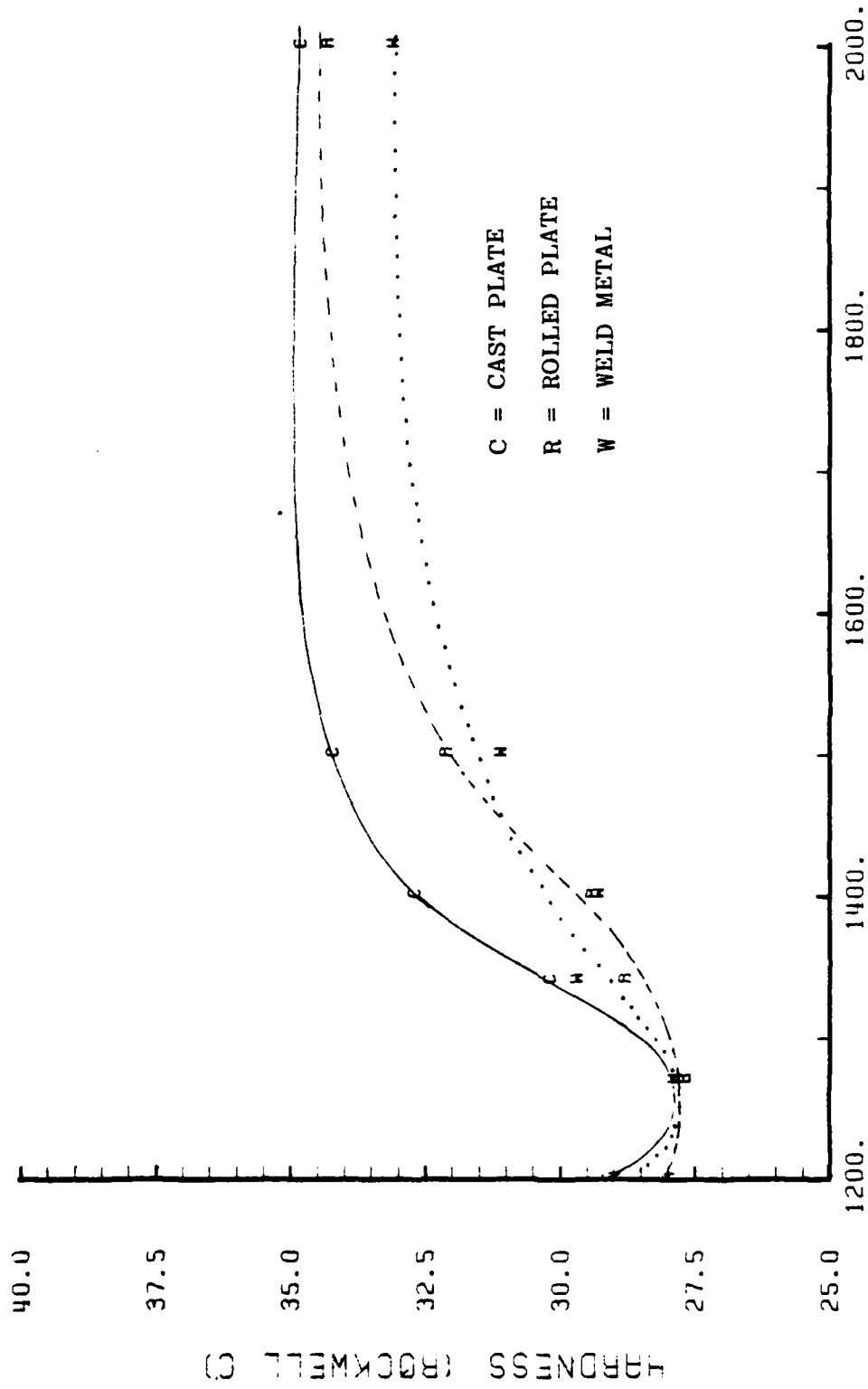
AUSTENITIZING TEMP (F) P = 13,000 (M)

Figure 19. Hardness vrs austenitizing temperature for temper group M



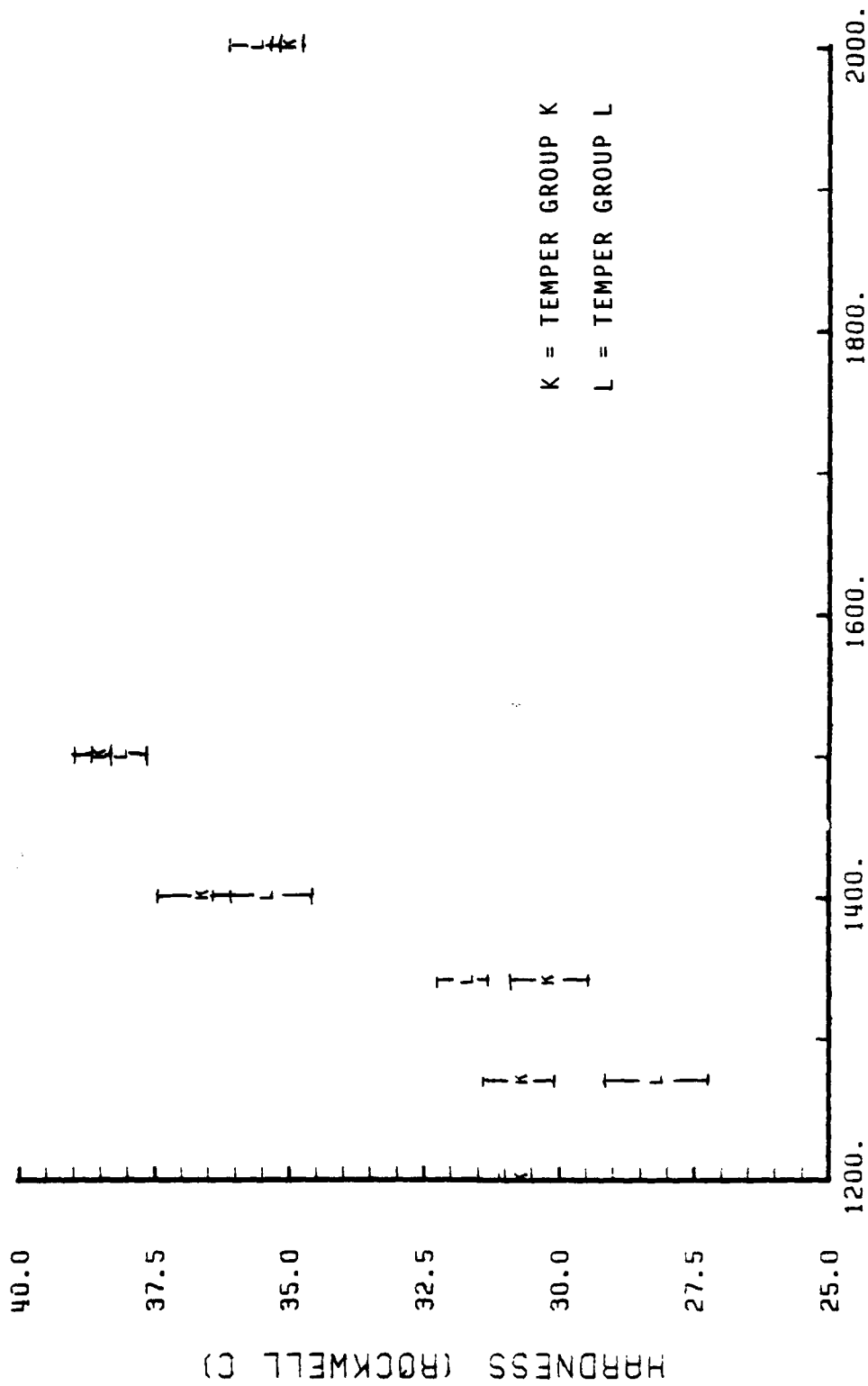
AUSTENITIZING TEMP (F) P = 13,000 (N)

Figure 20. Hardness vs austenitizing temperature for temper group N



AUSTENITIZING TEMP (F) P = 16,000 (0)

Figure 21. Hardness vrs austenitizing temperature for temper group 0



CAST PLATE AUSTENITIZING TEMP (F) P = 11,613

Figure 22. Comparison of cast plate temper groups K and L

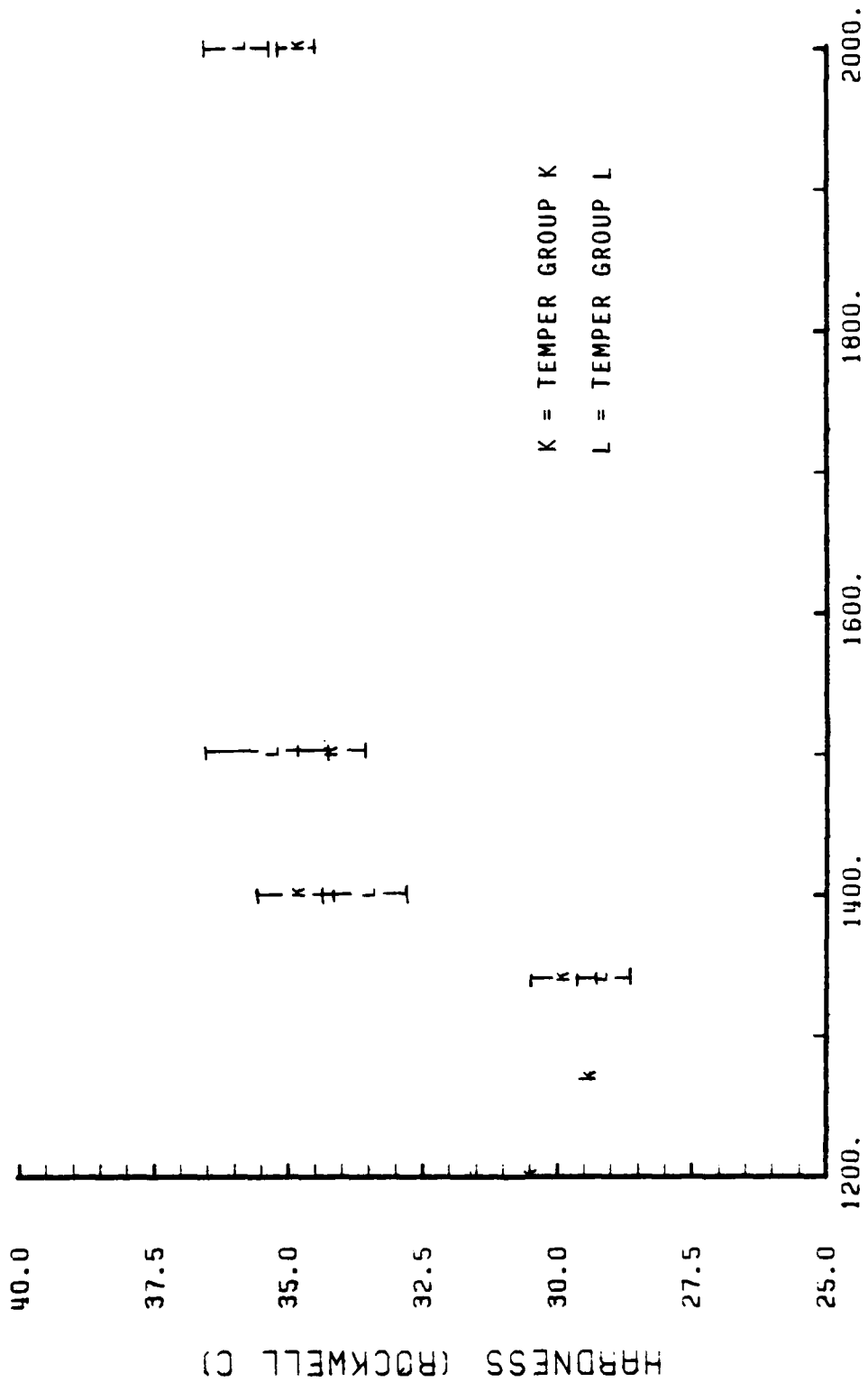
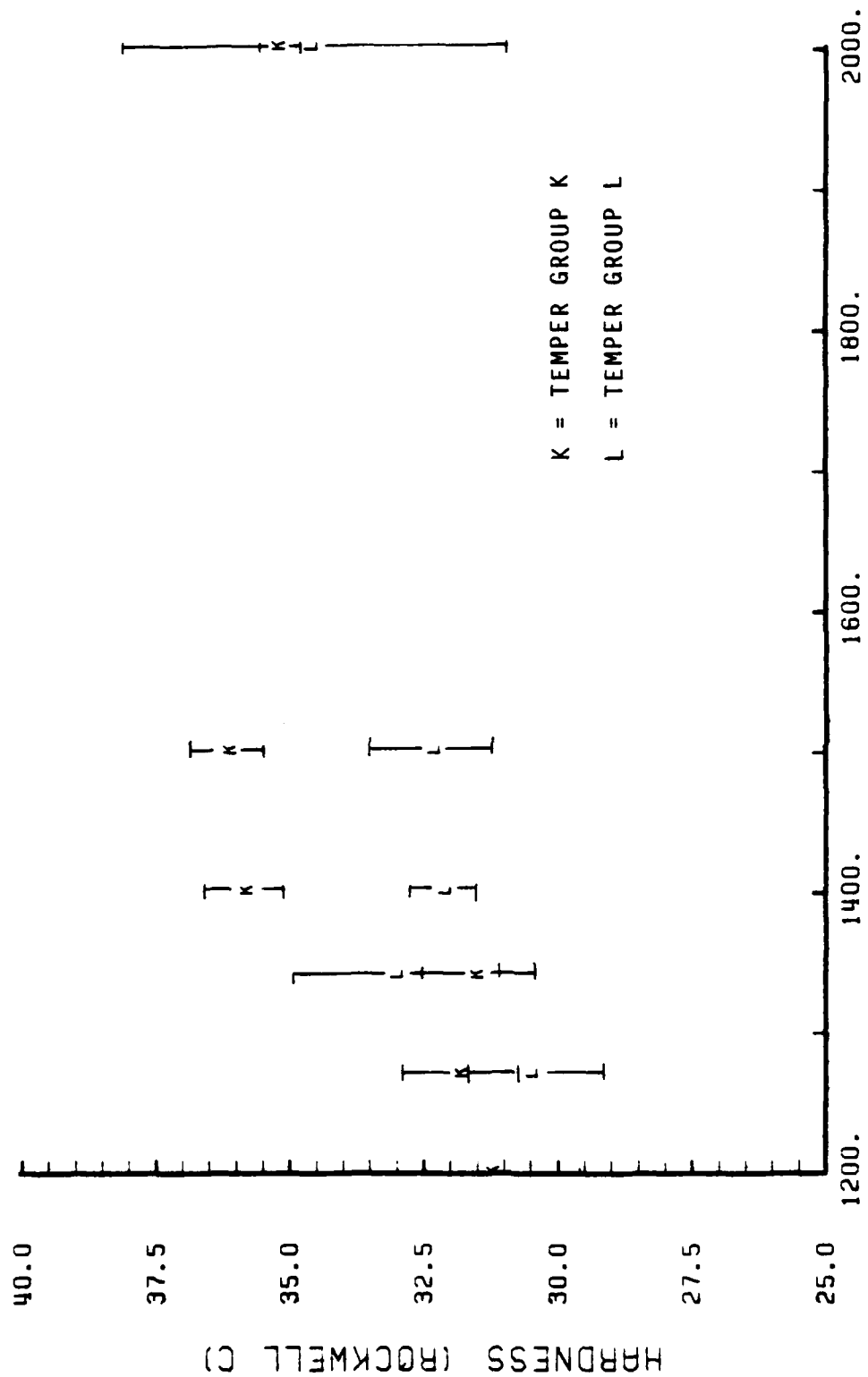


Figure 23. Comparison of rolled plate temper groups K and L

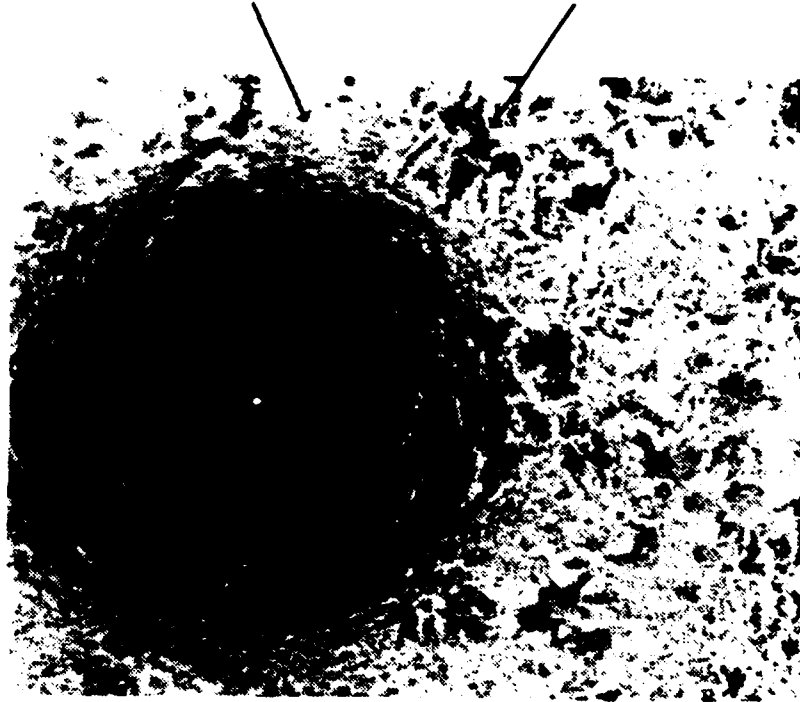


WELD METAL AUSTENITIZING TEMP (F) P = 11,613

Figure 24. Comparison of weld metal temper groups K and L

Untempered
Martensite

Darker Regions are the
As-received Tempered
Martensite



Austenitized at 1500^oF

56x

Figure 25. Rockwell C indenter

TABLE VIII
EFFECT OF DIFFERENT TEMPER
HARDNESS DIFFERENCE (ROCKWELL C) BETWEEN TEMPER GROUPS
J AND K

AUSTENITIZING TEMPERATURE (F)	J AND K		J AND L			
	h	R	C	W	K	C
2000	1.0	0.8	2.6	5.1	1.3	2.8
1500	0.0	2.5	-1.6	5.0	4.0	3.7
1400	N/A	0.5	0.4	4.9	5.9	4.3
1340	N/A	N/A	N/A	N/A	N/A	N/A

NOTE: W = WELD METAL, R = ROLLED PLATE, C = CAST PLATE
N/A = NOT AUSTENITIZED BASED ON METALLOGRAPHY

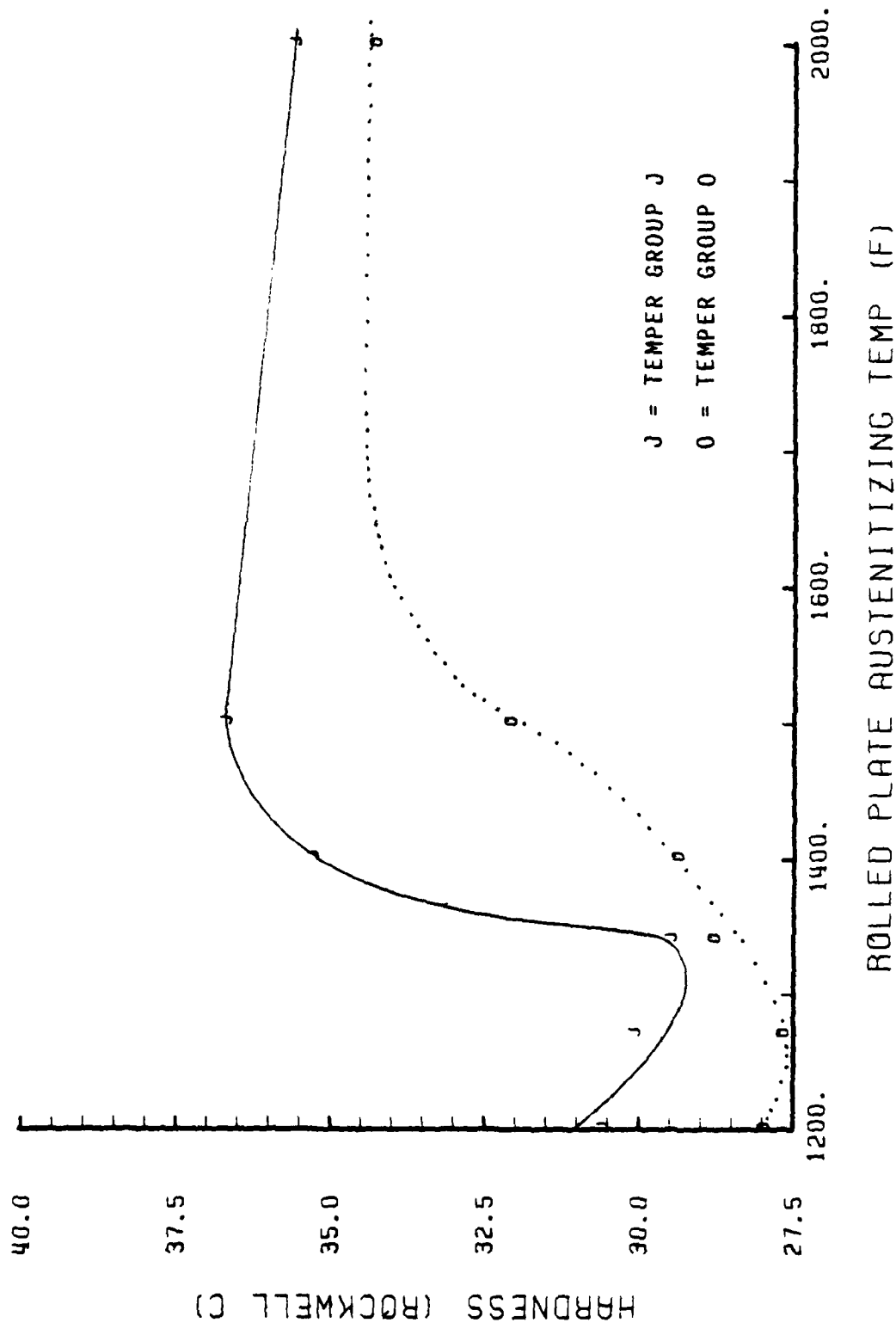
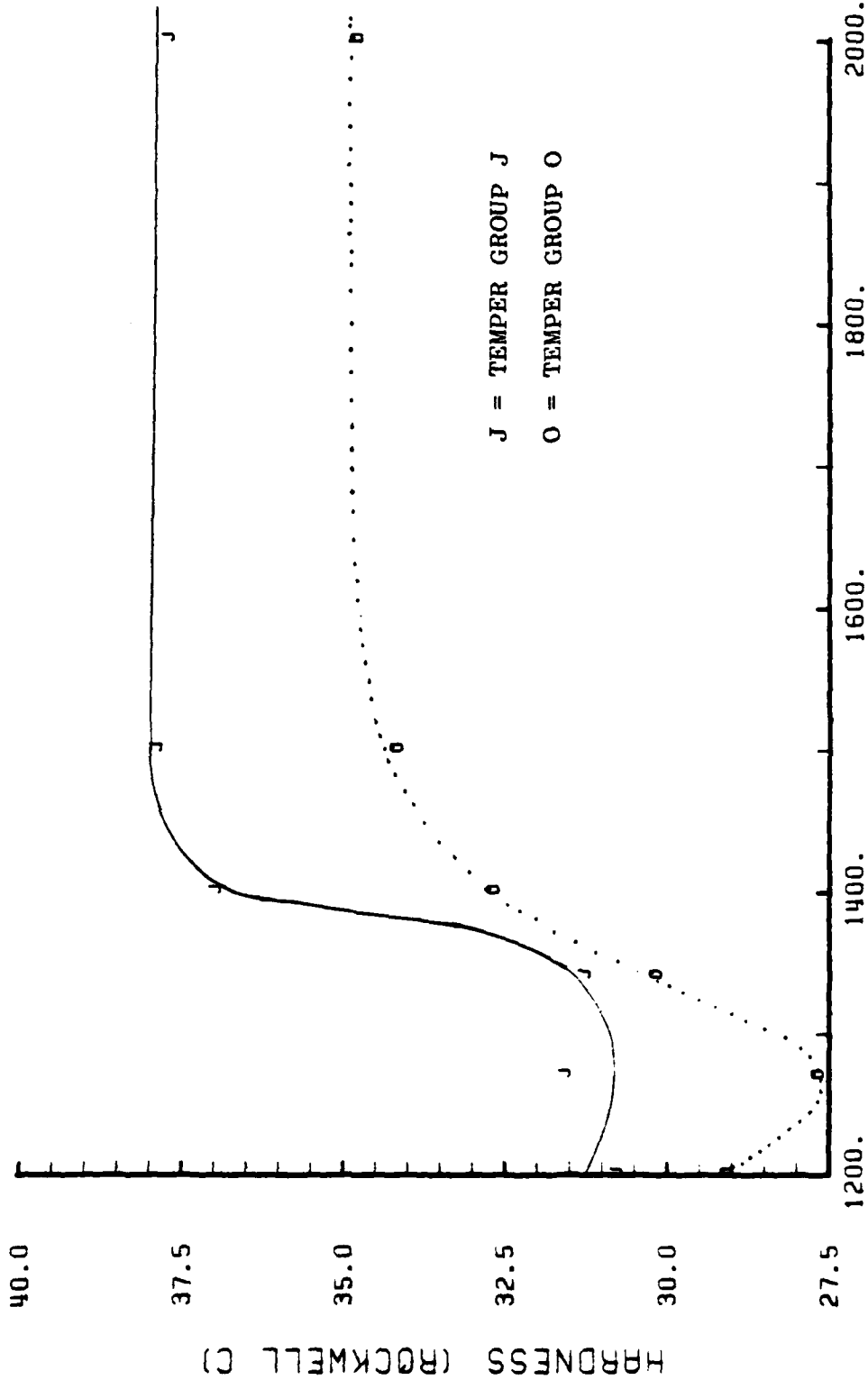


Figure 26. Comparison of rolled plate temper groups J and O



CAST PLATE AUSTENITIZING TEMP (F)

Figure 27. Comparison of cast plate temper groups J and O

LIST OF REFERENCES

1. Brucker, B. R., Fracture Properties of HY-130 Cast Plate Weldments, M. S. Thesis, Naval Postgraduate School, Monterey, CA, December 1980.
2. Hollomon, J. H. and Jaffe, L. D., "Time-Temperature in Tempering Steel", Transactions, American Institute of Mining and Metallurgical Engineers, v. 162, p. 223, 1945.
3. Grange, R. A. and Baughman, R. W., "Hardness of Tempered Martensite in Carbon and Low-Alloy Steels", Transactions, American Society for Metals, v. 48, p. 165, 1956.
4. Sorek, M., A Correlation between Heat Affected Zone Microstructures and the Thermal History During Welding of HY-130 Steels, M. S. Thesis, Naval Postgraduate School, Monterey, CA, September 1981.
5. Zanis, C. A. and Challenger, K. C., personal correspondence, January 1981.
6. Kellock, G. T. B., Sollars, A. R. and Smith, E., "Simulated Weld Heat-Affected Zone Structures and Properties of HY-80 Steel", Journal of the Iron and Steel Institute, December, 1971.

INITIAL DISTRIBUTION LIST

	No. Copies
1. Defense Technical Information Center Cameron Station Alexandria, Virginia 22314	2
2. Library, Code 0142 Naval Postgraduate School Monterey, California 93940	2
3. Department Chairman, Code 69 Department of Mechanical Engineering Naval Postgraduate School Monterey, California 93940	1
4. Assistant Professor K. D. Challenger, Code 69CH Department of Mechanical Engineering Naval Postgraduate School Monterey, California 93940	5
5. Dr. Charles Zanis, Code 2820 David Taylor Research and Development Center Annapolis, Maryland 21402	1
6. Mr. Ivo Fioritti, Code 323 Naval Sea Systems Command National Center, Building 3 2531 Jefferson Davis Highway Arlington, Virginia 20362	1
7. LCDR Paul E. Cincotta 500 Penhook Dr. Chesapeake, VA 23320	2
8. Mr. G. Power, Code 138.3 Mare Island Naval Shipyard Vallejo, California 94950	1

ATE
LMED
-8